

# 000 001 002 003 004 005 006 007 008 009 010 011 012 013 014 015 016 017 018 019 020 021 022 023 024 025 026 027 028 029 030 031 032 033 034 035 036 037 038 039 040 041 042 043 044 045 046 047 048 049 050 051 052 053 TASK-AWARE MECHANISM: HYBRID MoE VISION TOWER TOWARDS HOLISTIC VIDEO UNDERSTANDING

Anonymous authors

Paper under double-blind review

## ABSTRACT

Does *Comprehending the main idea of a 2-hour movie* and *Counting the birds appearing in a 15-second clip* really warrant the same video processing pipeline? Recent successes of Mixture-of-Experts (MoE) architectures in language modeling have inspired explorations of MoE applications. However, existing MoE models mainly focus on Large Language Models (LLMs) while neglecting Vision Tower (VT) in multimodal models. MoE-LLMs are predominantly designed for capacity scaling, whereas VT contains three fundamentally distinct modules, indicating that directly copying MoE-LLM designs to VT is unlikely to be effective. Inspired by the emerging Task-Aware idea, we argue that MoE-VT architectures should embody the principle of *Right Tool for the Right Job*, providing suitable processing to different tasks. To address this, we propose Task-Aware Mechanism (TAM), a MoE-VT architecture that employs Hybrid Gating Strategy to endow VT with intrinsic Task-Aware ability. To equip the framework with task-aware capabilities, we further introduce a compact Inductor module with only 0.1B parameters, trained on our new dataset TA-116k. With the Inductor, TAM could dynamically determine the appropriate task category, the optimal resolution and number of frames to sample, based on the user query and the length of video. Leveraging TAM, we introduce the TallVA-8B-A7B model, which outperforms current SOTA methods across various benchmarks on comparable LLMs, demonstrating that TAM enables video understanding models to become more holistic on diverse tasks.

## 1 INTRODUCTION

The recent breakthroughs in large language models (LLMs) OpenAI (2023); Group (2025) have sparked the emergence of large vision-language models (LVLMs) Zhang et al. (2024c); Yang et al. (2023); Bai & Keqin Chen (2025); Hong et al. (2024), which integrate visual and linguistic capabilities for vision-centric multimodal understanding. Influenced by the Scaling Law of LLM Kaplan et al. (2020), traditional paradigms in LVLMs have focused on improving performance through scaling up model with more parameters. However, larger single-model LVLMs often consume multiples of computational resources compared to smaller counterparts, yielding marginal performance gains. The success of Mixture-of-Experts (MoE) architectures has challenged the conventional preference for monolithic models. More crucially, MoE has reignited interest in the concept of Task-Aware idea Li et al. (2024c); Ranasinghe et al. (2024); Tan et al. (2024); Ataallah et al. (2024).

Task-Aware can be defined as "within a unified model architecture, the ability to perceive distinct task characteristics, dynamically select optimal tools, experts or processing pipelines, and achieve better performance with less or comparable activation parameters". Interpretable MoE architectures, frame-selection methodologies Ranasinghe et al. (2024); Tan et al. (2024) in video understanding models, and token-selection strategies, they collectively embody Task-Aware idea.

Current LVLMs have widely adopted sparse MoE architecture for LLM (MoE-LLM) Zhang et al. (2024a); Lin et al. (2024a), proven effective in scaling LLM capacity. However, research on the Vision Tower (VT) remains under-explored and lacks systematic exploration. As the "eye of LVLMs", the VT, typically composed of a Vision Encoder(VE), frame processing pipelines, and Projector, critically determines the quality of visual information available to LLM. A few attempts Zhang et al. (2024a); Riquelme et al. (2021); Li et al. (2024b) have replicated MoE-LLM designs to scale VT parameters, yielding only marginal gains, indicating that merely expanding capacity is insufficient.

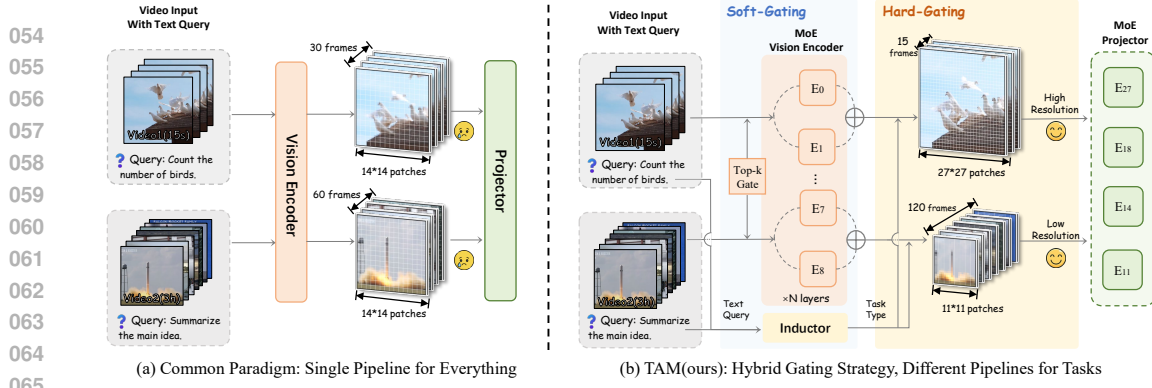


Figure 1: **Comparison of common paradigms (a) and TAM (b).** (a) Common paradigms, they usually have single pipeline for all tasks, such as  $\text{max\_fps}=2$  and  $\text{max\_frame}=60$ . (b) TAM utilizes Inductor to perceive video length and user query, then assigns appropriate frame numbers and resolutions for different tasks.

The main issue lies in the rigid visual processing paradigm of conventional VTs: all videos are uniformly converted into frame sequences with a fixed count and resolution, as shown in Fig. 1(a). It neglects the decisive role of the User Query in defining task requirements. For the same video, different queries may demand entirely different visual information—some requiring high-resolution frames for fine-grained recognition, while others need high-frame-rate for temporal dynamics.

This analysis reveals that the key to advancing LVLMs lies in developing a task-aware VT. Such a VT should adaptively decide video processing strategies based on the user query's intent, providing proper visual frames to LLM. The MoE paradigm, which advocates routing inputs to specialized experts, aligns naturally with this task-aware insights. To design an efficient, suitably gated MoE mechanism for different components in VT, there're two critical challenges:

**(1) Lack of Datasets.** Open-source dataset categorizing visual task metadata (e.g. user queries, video duration, resolution) doesn't exist. Former efforts mainly focus on semantic classification without considering task-specific visual requirements.

**(2) Lack of Adaptive Gating Strategies.** Since VT contains discrete stages, traditional Soft-Gating MoE strategy could not be uniformly applied across all components. For instance, recent work has demonstrated success by employing Hard-Gated VE for diverse feature extraction tasks, suggesting that Hard-Gating based on task-type may be available. Soft-Gating, as shown in Fig. 3(a), improves the stability of VE, whereas Hard-Gating, as illustrated in Fig. 3(b), demonstrates superior capability in detecting task types. Employing either strategy in isolation appears to be suboptimal.

To address these challenges, we propose Task-Aware Mechanism (TAM). There are three primary components in TAM. Task classification framework, and TA-116K datasets based on user query. A 0.1B text-only Inductor module that determines task types and the number of frames and resolution, according to user query and video length. And finally, the Hybrid Gated MoE-VT which provides tailored pipelines for different tasks. We summarize our primary contributions as follows:

- We introduce TAM, a Hybrid Sparse Gated MoE-VT architecture (Fig. 1(b)). We discover that MoE-ViT and Dynamic Frame Number & Resolution (DFR) exhibit strong synergy—neither component alone explains the performance gains, but their combination yields substantial improvements.

In our revised paper, we use Blue Bounding boxes like this to mark updated contents anonymously.

- We categorize video understanding tasks according to their sensitivity for frame count and resolution. We'll release TA-116K, 116K annotated queries from selected open-source datasets.
- Following TAM, we trained TallVA (Task Aware Large Language-Vision Assistant) with 8B total params and 7B activate params. When using comparable LLMs (Qwen2-7B, LLaMA3-8B, InternLM2.5-7B, etc.), TallVA outperforms the former SOTA across scenarios, even surpassing models based on much stronger LLMs in many benchmarks (Tab. 1), demonstrating the effectiveness of TAM and provide a reference for future research. We also visualize the results as radar chart Fig. 6.

We provide detailed cases of TallVA in Fig. 8. We envision our work inspiring future research on MoE design, and promoting Task-Aware idea to be applied to build more holistic multimodal models.

108 **2 RELATED WORK**

110 **Single LVLMs.** The evolution of LVLMs builds on vision-language alignment frameworks such  
 111 as Flamingo Alayrac et al. (2022) and BLIP-2 Li et al. (2023a), with the LLaVA series Liu et al.  
 112 (2023; 2024b;c); Zhang et al. (2024b); Li et al. (2024a) pioneering open-source models through  
 113 visual instruction tuning. Scaling efforts span stronger vision encoders Bai et al. (2023); Chen et al.  
 114 (2024b); Lin et al. (2023); Liu et al. (2024a), connector optimization Cha et al. (2024); Lin et al.  
 115 (2024b), and larger multimodal corpora McKinzie et al. (2024); Li et al. (2024d). Video extensions  
 116 Li et al. (2024c) tackle temporal modeling through token compression, but still face context window  
 117 limitations. Recent works further improve visual token efficiency via dynamic token merging Jin  
 118 et al. (2024), instruction-guided visual token pruning Huang et al. (2024), spectrum-preserving token  
 119 merging Tran et al. (2024), and adaptive positional encoding Zeng et al. (2024).

120 **MoE-LVLMs.** Mixture-of-Experts (MoE) architectures enhance LVLMs by conditional computation,  
 121 as seen in language models Fedus et al. (2022); Dai et al. (2024). MoE-LLaVA Lin et al. (2024a)  
 122 demonstrates the efficacy of sparse computation for visual reasoning, while DeepSeek-VL2 Wu et al.  
 123 (2024b) achieves modality-specific expert specialization. CuMo Li et al. (2024b) enables cross-modal  
 124 knowledge transfer via shared gating, and DynFocus Han et al. (2024) optimizes spatiotemporal  
 125 routing. Key challenges include load balancing and cross-modal routing, addressed through variance  
 126 regularization Zoph et al. (2022), contrastive learning Mustafa et al. (2022), and hierarchical routing  
 127 Gupta & Yip (2024). Moreover, Chen et al. (2023) explored the adaptive vision models.

128 **LVLMs with Task-Aware Insights.** Task-Aware has been gaining attention with the application  
 129 of MoE architecture, and the core idea is "Right Tool for the Right Job", aiming to find a proper  
 130 processing method for different tasks. Some video understanding models employ strategies to choose  
 131 suitable frames, and they meet Task-Awaring Insights well. Early methods used uniform sampling  
 132 Maaz et al. (2023) or relevance scoring Yu et al. (2023) in frames choosing, and modern approaches  
 133 include dynamic token compression Li et al. (2024c), lightweight frame selection Ranasinghe et al.  
 134 (2024); Tan et al. (2024), hierarchical processing Azad et al. (2025), and memory-augmented retrieval  
 135 Ataallah et al. (2024). MoE variants like DynFocus Han et al. (2024) and ChartMoE Xu et al. (2024)  
 136 enhance efficiency via specialized experts. Since Vision Tower(VT) hasn't received much attention,  
 137 improvements to VT will yield more performance gains at lower consistencies. In conclusion, as  
 138 a part that processes video directly, MoE-VT is more suitable to validate the Task-Aware idea. A  
 139 successful practice Wu et al. (2025) uses multiple Vision Encoders with different specifications to  
 help models get more information such as depth and color, making the model more holistic.

140 **3 METHODOLOGY**

141 **3.1 PRELIMINARY**

142 **MoE architecture.** The router assigns tokens to experts and calculates the weight matrix  $W \in \mathbb{R}^{N \times M}$ , where  $N$  and  $M$  represent the number of tokens and experts, respectively. In the Dense MoE  
 143 method, each token is assigned to all experts, and the output  $O$  is computed as:

$$144 \quad O_i = \sum_{j=1}^M W_{i,j} E_j(I_i), \quad O \in \mathbb{R}^{N \times D_{\text{out}}} \quad (1)$$

145 Here,  $E_j$  denotes the  $j$ -th expert,  $D$  denotes the dimension, and  $I \in \mathbb{R}^{N \times D_{\text{in}}}$  is the input. To reduce  
 146 computational costs, the Sparse MoE method assigns each token to only the top- $K$  experts with the  
 147 highest weights. The recalculated weight matrix is:

$$148 \quad W' = \text{Softmax}(\text{TopK}(W)), \quad W' \in \mathbb{R}^{N \times M} \quad (2)$$

149 Here,  $\text{TopK}(W)$  retains only the top- $K$  elements in each row of  $W$ , setting all other elements to zero.

150 **Weight Initialization and Gating Strategy.** Former MoE models initialize their experts with unique  
 151 weights, while Co-upcycling He et al. (2024); Komatsuzaki et al. (2023) initializes all experts with  
 152 the same weights derived from a pre-trained checkpoint. Soft-gating employs a trainable network to  
 153 compute  $W$ , offering high performance but increasing training complexity; in contrast, hard-gating  
 154 uses algorithms to compute  $W$ , simplifying training and facilitating hypothesis validation (Fig. 3).

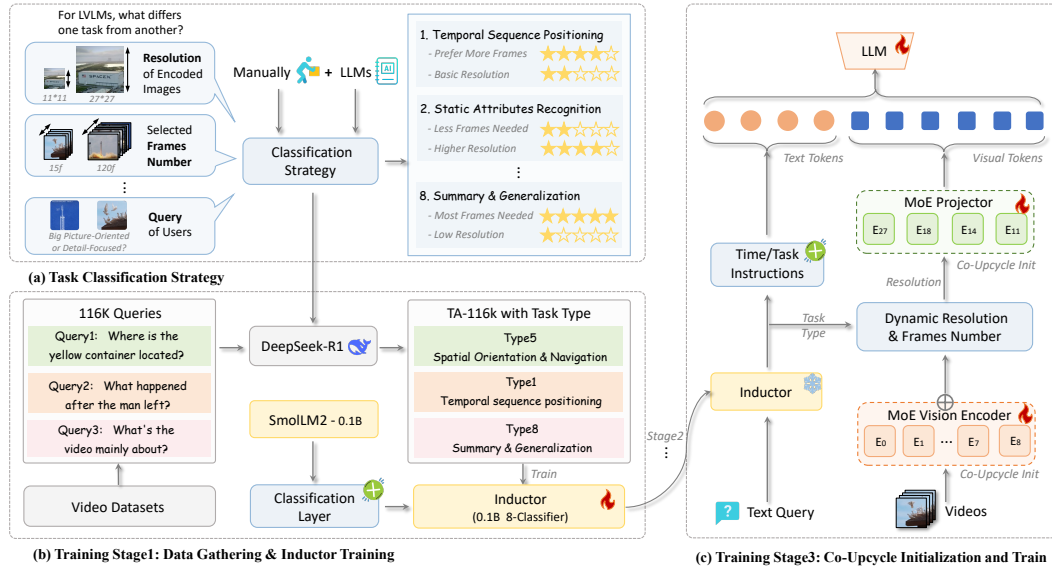


Figure 2: **Overview of our work.** (a) Considering video infos and user queries, we organized about 10k pieces of data and came up with 8 task classifications, according to their different sensitivities to resolution and frame number. (b) In the training stage 1, we use classification strategies to organize 116k queries and label them with Deepseek-R1 then train the Inductor. (c) Training stage 3. LLM has been adapted to Dynamic Frames after stage 2, then we initialize the VE and Projector in MoE-VT by Co-Upcycle Initialization and train.

### 3.2 TASK-AWARE MECHANISM

**Classification strategy.** Fig. 2(a). We collected 10k representative queries from various video understanding datasets Zhang et al. (2024c); Chen et al. (2024a); Farré et al. (2024); Rawal et al. (2024); Share (2024); Maaz et al. (2024). We classify the tasks into 8 categories according to their intrinsic meaning and, most importantly, their sensitivity to resolution and frame number. These categories are not mutually exclusive, as many tasks exhibit multiple attributes simultaneously. For example, Temporal Sequence Positioning is much more sensitive to the number of frames than resolution, while the task of Text Recognition (OCR) prefers higher resolution than frame number. Further implementation details are provided in Appendix A.

**Inductor and Dynamic Frames Choosing.** Fig. 2(b). As outlined in the Introduction, to develop a more robust router capable of considering both query and video length, we designed the Inductor. Specifically, we chose a lightweight pre-trained text model, SmollM2-135M-Instruct Allal et al. (2025), as the base model for the Inductor. The last layer of the Inductor is not the typical lm-head for text output, but a sequence classification layer capable of giving Softmax probabilities array.

In previous paradigms, all tasks shared the same frame processing pipeline. Videos are first subjected to uniform frame sampling and fed into the VE, followed by spatial pooling of the patch outputs(e.g., from  $27 \times 27$  to  $14 \times 14$ ), and finally to the LLM through Projector. Since we have established a task categorization strategy and systematically analyzed their sensitivity to resolution and frame count, we leverage this to dynamically allocate different frame numbers and resolutions across tasks. Specifically, given a fixed maximum context length, the upper bound for frame count is set to 120 following previous works, while each frame maintains a resolution of  $R \times R$ .

**Hybrid Sparse Gating Strategy.** Fig. 2(c). We apply the Sparse Soft-Gating MoE Strategy for the VE. Given that VE employs transformer architecture, the Soft-Gated design effectively enhances stability when handling complex tasks. For the projector, we employ Hard-Gating Resolution-specific Projectors, each designed exclusively for a particular resolution. This Hybrid Gating Strategy is also shown in Fig. 1(b). Through ablation studies in Sec. 4.3 and Tab. 3, we demonstrate that our Hybrid Gating Strategy maintains low activated parameters, taking the distinct characteristics of the VE and Projector into account, enhancing overall performance.

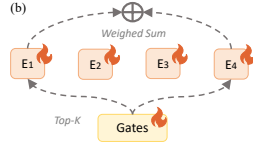
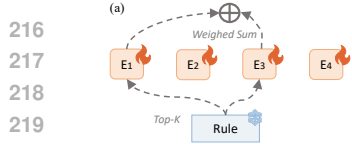


Figure 3: **Different gating strategies.** (a) Hard gating strategy with rules. (b) Soft gating strategy with router.

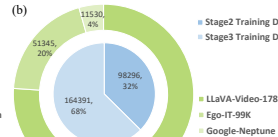
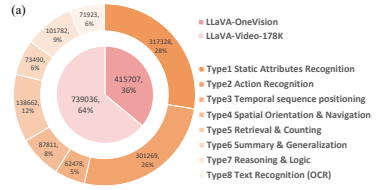


Figure 4: **Dataset Composition.** (a) In stage 1, the inner chart illustrates data source distribution, while the outer chart depicts 8-class distribution. (b) In stages 2-3, the inner chart compares train data allocation between consecutive stages, and the outer chart demonstrates relative contribution proportions from different data sources.

### 3.3 THREE-STAGE TRAINING RECIPES

**Data Collecting and Inductor Training.** In stage 1(Fig. 2(b)), we train the Inductor with our TA-116K dataset. We select 116K queries from open-source datasets Li et al. (2024a); Zhang et al. (2024c), then annotate these queries with the classification strategy and Deepseek-R1 DeepSeek-AI (2025), the details of annotation can be found in Appendix A. Each element is a pair as *(text query, classification label)*. Fig. 4(a) shows the distribution of data, and the details of the Inductor training sets can be found in Appendix E and Sec. 4.1.

**Training LLM to Adapt Dynamic Frame Number/Resolution.** In Stage 2, we surprisingly find that the LLM should be trained prior to the Projector in TAM, contrary to the classical paradigm Li et al. (2024a); Liu et al. (2023; 2024b;c) where Projector training is conducted first to align the vision side with the LLM. After multiple unsuccessful attempts using standard methodologies, we achieved improved results by prioritizing LLM training at this stage. This represents an interesting training paradigm, which we will comprehensively investigate in Sec. 4.3.

**MoE Initialization and Training.** In stage 3(Fig. 2(c)), we train all components of TallVA except the Inductor (trained in stage2, Fig. 5). The MoE initialization is performed through Co-Upcycle approach, namely, we duplicate each MLP layer in the VE in Stage 2 four times and append randomly initialized gating networks. Meanwhile, the Projector is also replicated 4 times and configured to process four distinct input resolutions separately. This implementation results in a Soft-Gating architecture for the VE and a Hard-Gating mechanism for the Projector. For the Soft-Gated VE, we incorporate an auxiliary loss function to ensure a balanced workload distribution, with technical details presented in Sec. 4.1. The training data composition and proportions across Stages 2-3 are illustrated in Fig. 4(b) , where Stage 3 accounts for 68% of the total training data.

## 4 EXPERIMENT

We train TallVA with a mixture of open-source datasets, which is demonstrated in Fig. 4, then we conduct comprehensive evaluation to verify its performance with various benchmarks and ablation studies. We also perform qualitative analysis, providing visualization charts and cases.

### 4.1 IMPLEMENTATION DETAILS

As illustrated in Fig. 4, we use essentially the same training data as the baseline, with minimal additional data to prevent overfitting (details in Appendix B).



Figure 5: **Training Stage 2**, train LLM to adapt dynamic frames choosing strategy before train all parts.

270 **Table 1: Comparisons between TallVA and other SOTA LVLMs on competitive benchmarks.** **Boldface**  
 271 indicates the highest score, and underlined scores denote the second-highest. All scores are averaged over at  
 272 least 3 runs. Models marked with  $\dagger$  employ more powerful LLMs(Qwen2.5-7B, Qwen2-72B Qwen-Team (2025;  
 273 2024)); we gray them out to ensure fair comparison. Scores with  $*$  outperform the models with stronger LLM.

Model-Params	General Video Understanding					Temporal Reasoning		Long Video Understanding		
	ActivityNet-QA	MVbench	Videommre w/o sub	Egoschema test	PerceptionTest	NeXTQA	TempCompass	LongVideoBench	MLVU val	MLVU test
NVILA-8B $\dagger$	60.9	68.1	64.1	54.3	65.4	82.2	69.7	57.7	-	49.5
LLaVA-OneVision-72B $\dagger$	60.8	56.7	66.2	62.0	66.9	79.4	67.1	63.2	66.4	47.2
<b>VideoLLama2.1-7B</b>	53.0	57.3	<b>54.9</b>	53.1	<b>54.9</b>	75.6	<b>56.8</b>	-	<b>57.4</b>	32.7
<b>Qwen2-VL-7B</b>	<u>57.4</u>	<b>66.0</b>	63.2	<u>66.7</u>	62.3	81.2	65.8	55.6	<u>69.4</u>	-
<b>InternVL2-8B</b>	56.3	63.1	58.6	-	63.5	82.5	66.0	54.6	64.0	38.4
<b>LLaVA-OneVision-7B</b>	56.6	56.7	58.2	60.1	57.1	79.4	64.2	56.3	64.7	<u>46.9</u>
<b>LLaVA-Video-7B</b>	56.5	58.6	<u>63.3</u>	57.3	<u>67.9</u>	<u>83.2</u>	65.4	<u>58.2</u>	<b>70.8</b>	44.8
<b>MiniCPM-V-2.5-8B</b>	56.1	62.3	60.9	64.5	64.4	80.3	<u>66.2</u>	56.1	66.8	41.7
<b>TallVA-8B-A7B(Ours)</b>	<b>61.3*</b>	<u>64.5</u>	<b>65.6</b>	<b>75.9*</b>	<b>69.1*</b>	<b>84.0*</b>	<b>68.8</b>	<b>59.6*</b>	68.5	<b>53.4*</b>

288 Following the Baseline, We use Siglip-400M as VE, two-layer MLP as Projector, and Qwen2-7B as  
 289 LLM. Full settings and hyperparameters can be found in Appendix E. The learning rate follows:

$$LR = LR_0 \cdot \sqrt{BS/BS_0} \quad (3)$$

293 where we set 2.5e-5 for LLM and 5e-6 for VE. To achieve load balance in MoE-VE, we use auxiliary  
 294 losses Zoph et al. (2022), where  $\mathcal{L}_{\text{ori}}$  is the next-token prediction loss,  $\alpha_b = 1e-3$ ,  $\alpha_z = 5e-4$ :

$$\mathcal{L} = \mathcal{L}_{\text{ori}} + \alpha_b \mathcal{L}_b + \alpha_z \mathcal{L}_z \quad (4)$$

## 4.2 MAIN RESULTS

300 **Comparison with former SOTA LVLMs that Use Same LLM.** In Tab. 1, we compare TallVA  
 301 with previous SOTA models, and we also present a radar chart(Fig. 6) to visualize the outstanding  
 302 performance of TallVA. We selected 10 challenging tasks Fu et al. (2024); Li et al. (2023b); Mangalam  
 303 et al. (2023); Xiao et al. (2021); Pătrăucean et al. (2023); Yu et al. (2019); Zhou et al. (2024); Wu et al.  
 304 (2024a); Liu et al. (2024d) spanning 3 evaluation categories: General Video Understanding, Temporal  
 305 Reasoning, and Long Video Understanding. For benchmarks containing open-ended questions, we  
 306 use GPT-3.5-turbo-1106 to compute the average score of multiple evaluations, following the settings  
 307 of the baseline. All the other data presented in Tab. 1 are sourced from either the GitHub pages or the  
 308 leaderboards of corresponding benchmarks. Overall, TallVA achieves superior results on the majority  
 309 of benchmarks, surpassing all models that employ the same LLM.

310 **Comparison with LVLMs that Use Stronger LLM.** Notably, we also compare TallVA against  
 311 current open-source SOTA video understanding models presented in the gray-shaded section of  
 312 Tab. 1. These models employ much stronger LLMs compared to Qwen2-7B, with some even utilizing  
 313 extensive private datasets. The evaluation scores highlighted in green in Tab. 1 demonstrate that  
 314 TallVA surpasses at least two strong baseline models. This remarkable performance validates the  
 315 effectiveness of the Task-Aware design in constructing our MoE-VE framework.

316 **Synergy of MoE and DFR.** A natural question is whether improvements stem from MoE capacity or  
 317 query-aware routing. As shown in Tab. 3(e), MoE-ViT alone *decreases* performance ( $-2.7\%$ ), while  
 318 DFR alone yields modest gains ( $+2.8\%$ ). However, combining MoE with DFR produces substantial  
 319 improvements (**+12.1%**). This synergy suggests that MoE experts specialize effectively only when  
 320 receiving task-appropriate visual inputs via DFR. Additional MoE isolation experiments are provided  
 321 in Appendix I. This is an important phenomenon we observed in our experiments, which indicates  
 322 that the combination of DFR and MoE-VE allows the MoE-VE with more parameters to achieve  
 323 significant performance improvements on tasks with different frame rates and resolutions.

324  
325  
326  
327  
328  
329  
330  
331  
332  
333  
334  
335  
336  
337  
338  
339  
340  
341  
342  
343  
344  
345  
346  
347  
348  
349  
350  
351  
352  
353  
354  
355  
356  
357  
358  
359  
360  
361  
362  
363  
364  
365  
366  
367  
368  
369  
370  
371  
372  
373  
374  
375  
376  
377  
Table 2: Discussion on Inductor performance and efficiency of TallVA.

Model - Param	Acc	Time
<i>SmolLM - 135M</i>	86.5%	61.0 s
<i>SmolLM2 - 135M</i>	91.7%	55.9 s
<i>SmolLM2 - 360M</i>	93.5%	78.4 s
<i>Qwen2.5 - 0.5B</i>	92.6%	101.2 s

Model	LLaVA-Video-7B	Qwen2-VL-7B	TallVA-A7B
<i>FLOPs</i>	$1.0844 * 10^{17}$	$1.1732 * 10^{17}$	$1.1976 * 10^{17}$

(b) Study of models' efficiency. The efficiency of TallVA is comparable to other LVLMs based on Qwen2-7B.

top-k in 4	k=1	k=2	k=4
<i>FLOPs</i>	$1.1519 * 10^{17}$	$1.1976 * 10^{17}$	$1.2603 * 10^{17}$

(c) Study of efficiency on different experts numbers.

331  
332  
333  
334  
335  
Table 3: Ablation studies for different training stages and components of TallVA.

	MV Bench	Videomm	MLVU-test
<i>Baseline (no training)</i>	58.6	62.3	44.8
+ Dynamic Frames Number & Resolution	59.3	63.2	45.2
+ Time/Task Instruction in Prompt	59.2	63.5	44.9
+ combination of the above two	59.5	63.5	46.1

(a) Study for different methods in Stage 1(not trained).

	MV Bench	Videomm	MLVU-test
<i>TallVA after stage 1</i>	59.5	63.5	46.1
+ train LLM only	61.8	64.4	48.5
+ train Projector only	57.9	62.8	42.2
+ train VE and Projector	48.3	59.1	32.7

(b) Study of Training Priorities in Stage 2.

	MV Bench	Videomm	MLVU-test
<i>TallVA after stage 2 (single Projector)</i>	61.8	64.4	48.5
+ soft MoE-VE (top2 in 4)	63.9	65.1	50.7
+ hard MoE-VE, based on task type	56.4	58.7	35.6
+ soft MoE-VE (top2 in 8)	63.2	63.8	50.0

(c) Routing Strategies for Vision Encoder.

	MV Bench	Videomm	MLVU-test
<i>TallVA after stage 2 (single VE)</i>	61.8	64.4	48.5
+ soft MoE-Projector (top2 in 4)	61.9	64.0	48.5
+ soft MoE-Projector (top2 in 8)	61.6	63.8	48.2
+ hard MoE-Projector, based on resolution	62.6	64.7	49.3

(d) Routing Strategies for Projector.

	ActivityNet-QA	MV Bench	MLVU-Test	Avg Change
<i>Baseline</i>	56.5	58.6	44.8	+0%
+ soft MoE-VE (top2 in 4)	55.4	56.7	43.5	-2.7%
+ Dynamic Frames Number & Resolution (DFR)	58.6	59.5	46.1	+2.8%
+ MoE / DFR (TallVA)	61.3	64.5	53.4	+12.1%

(e) The synergy of MoE and DFR produces effects far greater than using them individually.

### 4.3 ABLATION STUDIES

**Ablation Study in Stage 1.** In Stage 1, we trained the Inductor model, which serves as the core module of TAM for video duration-aware question classification. The Inductor receives both video duration information and user queries to determine question categories. Starting from the base model, we incrementally incorporated two key components: Dynamic Frames Number and Resolution (hereafter referred to as DFR), along with Time/Task Instruction. Through systematic ablation experiments as Tab. 3(a), we demonstrated the effectiveness of these enhancements.

**Ablation Study of Training Priorities in Stage 2.** As mentioned in Sec. 3.3, we prioritize LLM training in Stage 2(Fig. 5). Since the common paradigms Li et al. (2024a); Liu et al. (2023; 2024b;c) either trained the Projector or trained the entire VT first, this finding surprised us. While training the Projector in Stage 2 was expected to enhance performance, we observed significant performance degradation instead. Through ablation experiments as Tab. 3(b), we argue that the LLM was most profoundly impacted by Dynamic Frames, since it had previously only handled fixed frame numbers and resolutions. The loss curve under different training methods can be found in Appendix H.

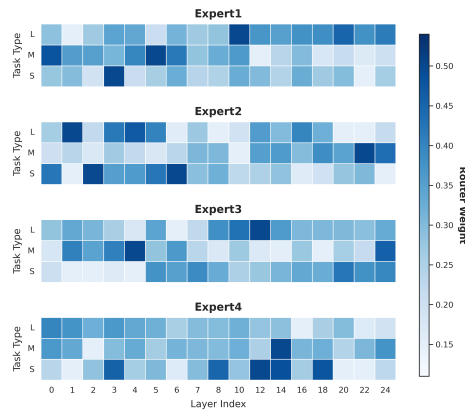
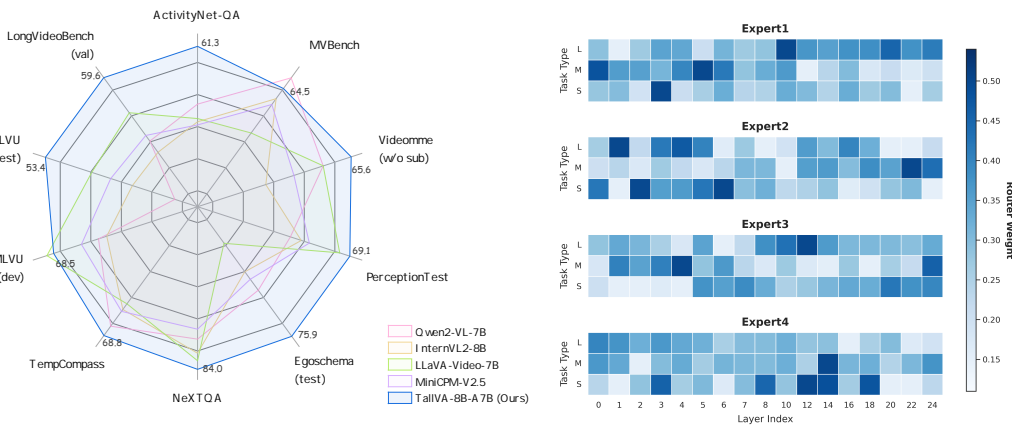
**Study on Gating Strategies for VE and Projector.** We demonstrate that in models like TAM, the VE achieves better performance improvements when employing Soft-Gating. In contrast, implementing Hard-Gating based on task-type negatively impacts model stability, leading to performance degradation. Conversely, for the Projector module with only a limited number of layers, the benefits of Soft-Gating are limited compared to resolution-based routing mechanisms. Experimental results presented in Tab. 3(c) and Tab. 3(d) validate the effectiveness of our Hybrid Gating Strategy. Additionally, we provide expert-swap and routing-scramble experiments in Appendix I to demonstrate that MoE experts are not interchangeable.

378  
379  
380 Table 4: The robustness analysis of the Inductor module.  
381  
382  
383  
384  
385

Confidence	0–0.2	0.2–0.4	0.4–0.6	0.6–0.8	0.8–1.0	All
Inductor Acc	0.59	0.73	0.84	0.93	0.98	92.3%
TAM Acc	0.39	0.47	0.61	0.70	0.75	68.2%
Baseline Acc	0.36	0.45	0.56	0.63	0.67	63.1%
Sample Numbers	136	544	1679	5212	2429	10000
Percentage	1.4%	5.4%	16.8%	52.1%	24.3%	100%

386 (a) Calibration analysis on 10k held-out samples. TAM outperforms baseline across all confidence buckets.  
387

Methods	Original Data	Paraphrase@DS	Paraphrase@GPT
	Acc@Inductor	91.4%	90.2%

388 (b) Paraphrasing robustness. Minimal accuracy drop confirms generalization beyond specific phrasings.  
389  
390  
391

## 4.4 ROBUSTNESS ANALYSIS

**Inductor Selection and Calibration.** We selected three text-only pre-trained mini models as Inductor candidates (Tab. 2(a)). SmolLM2-135M demonstrated good efficiency while maintaining competitive accuracy. To assess potential cascading errors from misclassification, we evaluated calibration on 10k held-out samples. As shown in Tab. 4(a), the Inductor achieves 92% overall accuracy, and even in low-confidence regions (0–0.2), accuracy remains at 59%—well above nominal confidence.

**Confusion Matrix and ECE.** The confusion matrix can effectively show the training performance of the Inductor. We provide a detailed  $8 \times 8$  confusion matrix across all task types in Tab. 6, showing an average acc of 93%. We also compute the Expected Calibration Error (ECE):

$$ECE = \sum_i p_i \cdot |Acc_i - Conf_i| \quad (5)$$

where  $p_i$  is the proportion of samples in bucket  $i$ , and  $Conf_i$  is the average confidence. The ECE is 0.226, primarily driven by *under-confidence*, which is benign for routing. Importantly, TAM consistently outperforms the baseline across all confidence buckets.

**Fallback Strategies.** Though Inductor already has high accuracy, we still set up a Fallback Policy: there are minimum or max frame counts that scale with video length, and always provide explicit video metadata to the LLM, allowing TAM to handle videos of extreme lengths regardless of task-type predictions, ensuring the stability and generalization ability in edge cases. We provide many examples in Appendix C, showing that TAM is not simply a combination of 8 frame number/resolution types.

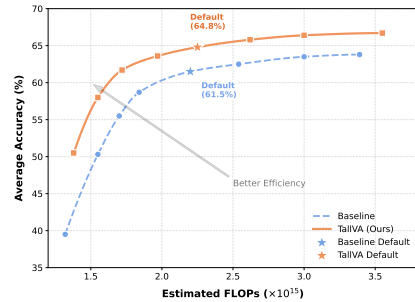
**Paraphrasing Experiments.** We conducted experiments on the Inductor with 1k queries paraphrased by DeepSeek-V3 and GPT-4o (Tab. 4(b)). The drop in accuracy is very small (about -1%), indicating good robustness and generalization ability of the Inductor and TAM.

432  
433  
434 Table 5: Scalability, data efficiency, and accuracy–efficiency analysis of our methods.  
435  
436

Method	EgoSchema (before)	EgoSchema (after)	Growth Rate
TallVA (8% EgoIT-99K)	57.3	<b>75.9</b>	<b>32.5%</b>
Baseline + 8% EgoIT-99K	57.3	71.4	24.6%
EgoGPT (15% EgoIT-99K)	60.1	73.2	21.8%

437  
438 (a) Data efficiency on EgoSchema.  
439

Model	Videomme	NextQA	LongVideoBench
LLaVA-Video-7B	63.3	83.2	58.2
LLaVA-Video-7B + TAM	64.1 (+0.8)	83.5 (+0.3)	58.7 (+0.5)
LLaVA-Video-72B	70.5	85.4	61.9
LLaVA-Video-72B + TAM	<b>71.9 (+1.4)</b>	85.5 (+0.1)	<b>63.1 (+1.2)</b>

440  
441 (b) Scalability to 72B LLMs via LoRA fine-tuning.  
442  
443444  
445 (c) Acc-FLOPs tradeoff. TallVA achieves  
446 higher accuracy at comparable FLOPs.  
447448 Table 6: **Confusion Matrix of Inductor across 8 Task Types.** We evaluated 200 unseen samples per class.  
449 Per-class accuracies range from 85.5% to 97%, with reasonable confusion between semantically similar tasks  
(e.g., Task 1 “Static Attr.” and Task 3 “Fine-grained Attr.”). Task indices can be found in Appendix A.  
450

Prediction \ GT	1	2	3	4	5	6	7	8
1	<b>92.5%</b>	3%	3.5%	0	1%	0	0	0
2	2.5%	<b>87.5%</b>	3%	3%	0.5%	0	2.5%	1%
3	1.5%	3%	<b>86.5%</b>	1.5%	2%	0	4.5%	1%
4	0	1.5%	2%	<b>94%</b>	0	2%	0.5%	0
5	0	0.5%	1%	0	<b>91.5%</b>	0	4%	3%
6	0	1%	0	0.5%	0.5%	<b>97%</b>	0	1%
7	3%	3.5%	4%	1%	1%	1%	<b>85.5%</b>	1%
8	0.5%	0	0	0	3.5%	0	3%	<b>93%</b>
<i>Total Acc.</i>	92.5%	87.5%	86.5%	94%	91.5%	97%	85.5%	93%

451  
452 4.5 GENERALIZATION ANALYSIS  
453  
454

455 **Scalability to Larger Models.** We applied TAM via LoRA to both LLaVA-Video-7B and 72B  
456 (Tab. 5(b)). Both models benefit, with notably larger gains for the 72B model on long-video  
457 benchmarks (+1.4% Videomme, +1.2% LongVideoBench). This indicates stronger LLMs may  
458 benefit more from TAM. We also demonstrate low-cost extensibility: defining a “very-long-video”  
459 task type with  $\sim 800$  samples and LoRA fine-tuning yields clear gains (details in Appendix I).

460 **Data Efficiency.** TallVA demonstrates remarkable data efficiency on EgoSchema (Tab. 5(a)). Using  
461 only 8% of EgoIT-99K data, TallVA achieves a 32.5% growth rate—significantly higher than the  
462 baseline (24.6%) and EgoGPT (21.8% with 15% data). This suggests that TAM’s architecture is more  
463 efficient at exploiting training data, and also indicates that TAM’s performance improvement mainly  
464 comes from architectural enhancements.

465  
466 4.6 LOAD BALANCE, EFFICIENCY AND CASE ANALYSIS  
467

468 **Experts Load Distribution.** In Fig. 7, we recorded the average routing weights of each expert across  
469 layers in MoE-VE. It illustrates that MoE-VE may have different expert allocation patterns for videos  
470 of varying lengths. “L/M/S” denotes Long(more than 180s)/Medium/Short(less than 30s) videos, and  
471 a higher weight indicates greater expert contribution at that layer. Simultaneously, in Appendix H,  
472 we provide the MoE-VE layer-wise visualization with load balancing Fig. 12b.

473 **Efficiency Analysis.** The increased number of parameters in TallVA primarily comes from the FFN  
474 parameters of Siglip-400M, which are replicated during upcycling. The efficiency of TallVA is  
475 comparable to other video understanding 7B LLMs. As shown in Tab. 2(b,c), TallVA’s FLOPs are  
476 comparable to dense models. Moreover, we visualized the accuracy–FLOPs tradeoff in Tab. 5(c):  
477 TallVA achieves higher accuracy at similar compute, and reaches target accuracy with fewer FLOPs.

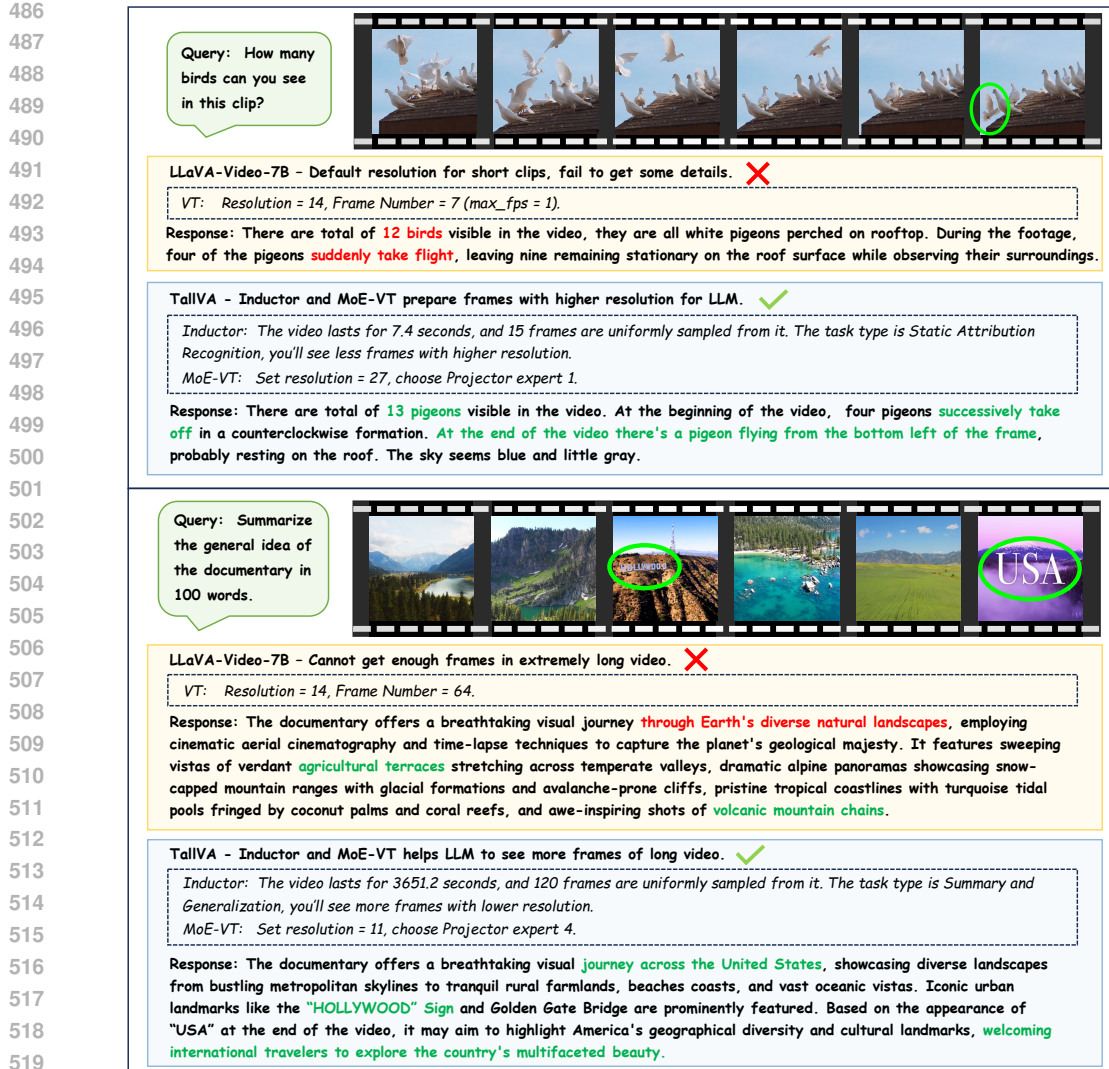


Figure 8: **Dialogues between User and Model on Challenging Tasks.** We highlight correct and incorrect content. We also visualize the outputs of Inductor and MoE-VT. More cases can be found in Appendix C.

**Case Study.** In Fig. 1 and Fig. 8, we demonstrate TallVA’s flexibility across different tasks. More cases and limitations are discussed in Appendix C and G. These complementary tasks show that TAM could effectively make the model more holistic, handling various real-world applications.

## 5 CONCLUSION

In this paper, we introduce Task-Aware Mechanism (TAM), a hybrid-gated MoE Vision Tower framework that dynamically adapts frame count and resolution based on user-queries. Our model TallVA surpasses previous SOTA models on the same-scale LLM.

- A key finding is that MoE-ViT and DFR exhibit strong synergy: using them individually only brings slight performance improvements, while their combination yields substantial gains (+12.1%), suggesting that MoE experts specialize effectively only when receiving task-appropriate visual inputs.
- We demonstrate that our 0.1B Inductor is well-calibrated, robust, and extensible to new task types in broad ablation studies from Tab. 2 to Tab. 6 and Appendix I. We also found that TAM can scale up for larger models, and achieves better accuracy-compute tradeoffs(Tab. 5).

TAM reveals a potential direction for the development of video understanding models. We hope this can inspire more follow-up work to jointly explore low-cost task-aware approaches.

540 ETHICS STATEMENT  
541

542 This work presents Task-Aware Mechanism (TAM) to improve multimodal expert models, with  
543 no immediately apparent ethical issues arising from the methodology itself. However, as with any  
544 advancement in large vision-language models (LVLMs), the open-release of models may entail  
545 broader societal implications. While a non-commercial license is applied to restrict misuse, the  
546 potential for dual-use or unintended applications remains. We encourage ongoing ethical evaluation  
547 to mitigate risks associated with the growing capabilities of multimodal AGI systems. Furthermore,  
548 we discussed the potential border impact in Appendix D.

549  
550 REPRODUCIBILITY STATEMENT  
551

552 In this paper, we strive to enhance the reproducibility of our work. The overall workflow is depicted  
553 in Fig. 2, and the detailed structure of the training dataset is illustrated in Fig. 4. Additionally, we  
554 provide comprehensive details of the experimental setup in Sec. 4.1, along with key hyperparameters  
555 listed in Appendix E. The supplementary materials include a code.zip file, which will be made  
556 publicly available in the future. We also plan to release the model weights and the TA-116k dataset.  
557 More details can be found in Appendix E and F.

558  
559 THE USE OF LARGE LANGUAGE MODELS (LLMs)  
560

561 Overall, our work utilizes LLMs to facilitate the creation of the TA-116K dataset, which is intended  
562 for training Inductor. In Fig. 2(a), we illustrate schematically how LLMs are employed in our  
563 approach; specifically, Sec. 3.2 describes the use of LLMs for annotating existing data, while the  
564 detailed prompts are provided in Appendix A. The above constitutes all aspects of our work that  
565 involve the application of LLMs.

566  
567 REFERENCES  
568

569 Jean-Baptiste Alayrac, Jeff Donahue, Pauline Luc, Antoine Miech, Iain Barr, Yana Hasson, Karel  
570 Lenc, Arthur Mensch, Katherine Millican, Malcolm Reynolds, et al. Flamingo: a visual language  
571 model for few-shot learning. *Advances in neural information processing systems*, 35:23716–23736,  
572 2022.

573 Loubna Ben Allal et al. Smollm2: When smol goes big – data-centric training of a small language  
574 model, 2025. URL <https://arxiv.org/abs/2502.02737>.

575 Kirolos Ataallah, Xiaoqian Shen, Eslam Abdelrahman, Essam Sleiman, Mingchen Zhuge, Jian  
576 Ding, Deyao Zhu, Jürgen Schmidhuber, and Mohamed Elhoseiny. Goldfish: Vision-language  
577 understanding of arbitrarily long videos. In *European Conference on Computer Vision*, pp. 251–267.  
578 Springer, 2024.

579 Shehreen Azad, Vibhav Vineet, and Yogesh Singh Rawat. Hierarq: Task-aware hierarchical q-former  
580 for enhanced video understanding. *arXiv preprint arXiv:2503.08585*, 2025.

581 Jinze Bai, Shuai Bai, Shusheng Yang, Shijie Wang, Sinan Tan, Peng Wang, Junyang Lin, Chang Zhou,  
582 and Jingren Zhou. Qwen-vl: A versatile vision-language model for understanding, localization,  
583 text reading, and beyond, 2023. URL <https://arxiv.org/abs/2308.12966>.

584 Shuai Bai and et al. Kefin Chen. Qwen2.5-vl technical report, 2025. URL <https://arxiv.org/abs/2502.13923>.

585 Junbum Cha, Wooyoung Kang, Jonghwan Mun, and Byungseok Roh. Honeybee: Locality-enhanced  
586 projector for multimodal ILM. In *Proceedings of the IEEE/CVF Conference on Computer Vision  
587 and Pattern Recognition*, pp. 13817–13827, 2024.

588 Lin Chen, Xilin Wei, Jinsong Li, Xiaoyi Dong, Pan Zhang, Yuhang Zang, Zehui Chen, Haodong  
589 Duan, Bin Lin, Zhenyu Tang, et al. Sharegpt4video: Improving video understanding and generation  
590 with better captions. *arXiv preprint arXiv:2406.04325*, 2024a.

594 Tianlong Chen, Xuxi Chen, Xianzhi Du, Abdullah Rashwan, Fan Yang, Huizhong Chen, Zhangyang  
 595 Wang, and Yeqing Li. Adamv-moe: Adaptive multi-task vision mixture-of-experts. In *Proceedings*  
 596 *of the IEEE/CVF International Conference on Computer Vision*, pp. 17346–17357, 2023.

597

598 Zhe Chen, Jiannan Wu, Wenhui Wang, Weijie Su, Guo Chen, Sen Xing, Muyan Zhong, Qinglong  
 599 Zhang, Xizhou Zhu, Lewei Lu, et al. Internvl: Scaling up vision foundation models and aligning  
 600 for generic visual-linguistic tasks. In *Proceedings of the IEEE/CVF conference on computer vision*  
 601 *and pattern recognition*, pp. 24185–24198, 2024b.

602 Damai Dai et al. Deepseekmoe: Towards ultimate expert specialization in mixture-of-experts language  
 603 models, 2024. URL <https://arxiv.org/abs/2401.06066>.

604

605 DeepSeek-AI. Deepseek-r1: Incentivizing reasoning capability in llms via reinforcement learning,  
 606 2025. URL <https://arxiv.org/abs/2501.12948>.

607 Miquel Farré, Andi Marafioti, Lewis Tunstall, Leandro Von Werra, and Thomas Wolf. Finevideo.  
 608 <https://huggingface.co/datasets/HuggingFaceFV/finevideo>, 2024.

609

610 William Fedus, Barret Zoph, and Noam Shazeer. Switch transformers: Scaling to trillion parameter  
 611 models with simple and efficient sparsity, 2022. URL <https://arxiv.org/abs/2101.03961>.

612

613 Chaoyou Fu et al. Video-mme: The first-ever comprehensive evaluation benchmark of multi-modal  
 614 llms in video analysis, 2024. URL <https://arxiv.org/abs/2405.21075>.

615

616 DeepSeek-AI Group. Deepseek-v3 technical report, 2025. URL <https://arxiv.org/abs/2412.19437>.

617

618 Nikhil Gupta and Jason Yip. Dbrx: Creating an llm from scratch using databricks. In *Databricks  
 619 Data Intelligence Platform: Unlocking the GenAI Revolution*, pp. 311–330. Springer, 2024.

620

621 Yudong Han, Qingpei Guo, Liyuan Pan, Liu Liu, Yu Guan, and Ming Yang. Dynfocus: Dynamic  
 622 cooperative network empowers llms with video understanding. *arXiv preprint arXiv:2411.12355*,  
 623 2024.

624

625 Ethan He, Abhinav Khattar, Ryan Prenger, Vijay Korthikanti, Zijie Yan, Tong Liu, Shiqing Fan,  
 626 Ashwath Aithal, Mohammad Shoeybi, and Bryan Catanzaro. Upcycling large language models  
 627 into mixture of experts, 2024. URL <https://arxiv.org/abs/2410.07524>.

628

629 Wenyi Hong et al. Cogvlm2: Visual language models for image and video understanding, 2024. URL  
 630 <https://arxiv.org/abs/2408.16500>.

631

632 Kai Huang, Hao Zou, Ye Xi, BoChen Wang, Zhen Xie, and Liang Yu. IVTP: Instruction-guided  
 633 visual token pruning for large vision-language models. In *European Conference on Computer  
 634 Vision*, pp. 214–230. Springer, 2024.

635

636 Peng Jin, Ryuichi Takanobu, Wancai Zhang, Xiaochun Cao, and Li Yuan. Chat-univi: Unified  
 637 visual representation empowers large language models with image and video understanding. In  
 638 *Proceedings of the IEEE/CVF Conference on Computer Vision and Pattern Recognition*, pp.  
 13700–13710, 2024.

639

640 Jared Kaplan, Sam McCandlish, Tom Henighan, Tom B. Brown, Benjamin Chess, Rewon Child,  
 641 Scott Gray, Alec Radford, Jeffrey Wu, and Dario Amodei. Scaling laws for neural language models,  
 642 2020. URL <https://arxiv.org/abs/2001.08361>.

643

644 Aran Komatsuzaki, Joan Puigcerver, James Lee-Thorp, Carlos Riquelme Ruiz, Basil Mustafa, Joshua  
 645 Ainslie, Yi Tay, Mostafa Dehghani, and Neil Houlsby. Sparse upcycling: Training mixture-of-  
 646 experts from dense checkpoints, 2023. URL <https://arxiv.org/abs/2212.05055>.

647

648 Bo Li, Yuanhan Zhang, Dong Guo, Renrui Zhang, Feng Li, Hao Zhang, Kaichen Zhang, Peiyuan  
 649 Zhang, Yanwei Li, Ziwei Liu, et al. Llava-onevision: Easy visual task transfer. *arXiv preprint  
 650 arXiv:2408.03326*, 2024a.

648 Jiachen Li, Xinyao Wang, Sijie Zhu, Chia-Wen Kuo, Lu Xu, Fan Chen, Jitesh Jain, Humphrey Shi,  
 649 and Longyin Wen. Cumo: Scaling multimodal llm with co-upcycled mixture-of-experts. *Advances*  
 650 *in Neural Information Processing Systems*, 37:131224–131246, 2024b.

651

652 Junnan Li, Dongxu Li, Silvio Savarese, and Steven Hoi. Blip-2: Bootstrapping language-image  
 653 pre-training with frozen image encoders and large language models. In *International conference*  
 654 *on machine learning*, pp. 19730–19742. PMLR, 2023a.

655

656 Kunchang Li, Yali Wang, Yinan He, Yizhuo Li, Yi Wang, Yi Liu, Zun Wang, Jilan Xu, Guo Chen,  
 657 Ping Luo, et al. Mvbench: A comprehensive multi-modal video understanding benchmark. *arXiv*  
 658 *preprint arXiv:2311.17005*, 2023b.

659

660 Yanwei Li, Chengyao Wang, and Jiaya Jia. Llama-vid: An image is worth 2 tokens in large language  
 661 models. In *European Conference on Computer Vision*, pp. 323–340. Springer, 2024c.

662

663 Yanwei Li, Yuechen Zhang, Chengyao Wang, Zhisheng Zhong, Yixin Chen, Ruihang Chu, Shaoteng  
 664 Liu, and Jiaya Jia. Mini-gemini: Mining the potential of multi-modality vision language models.  
 665 *arXiv preprint arXiv:2403.18814*, 2024d.

666

667 Bin Lin, Zhenyu Tang, Yang Ye, Jinfa Huang, Junwu Zhang, Yatian Pang, Peng Jin, Munan Ning,  
 668 Jiebo Luo, and Li Yuan. Moe-llava: Mixture of experts for large vision-language models, 2024a.  
 669 URL <https://arxiv.org/abs/2401.15947>.

670

671 Ji Lin, Hongxu Yin, Wei Ping, Pavlo Molchanov, Mohammad Shoeybi, and Song Han. Vila: On  
 672 pre-training for visual language models. In *Proceedings of the IEEE/CVF conference on computer*  
 673 *vision and pattern recognition*, pp. 26689–26699, 2024b.

674

675 Ziyi Lin, Chris Liu, Renrui Zhang, Peng Gao, Longtian Qiu, Han Xiao, Han Qiu, Chen Lin, Wenqi  
 676 Shao, Keqin Chen, et al. Sphinx: The joint mixing of weights, tasks, and visual embeddings for  
 677 multi-modal large language models. *arXiv preprint arXiv:2311.07575*, 2023.

678

679 Dongyang Liu, Renrui Zhang, Longtian Qiu, Siyuan Huang, Weifeng Lin, Shitian Zhao, Shijie Geng,  
 680 Ziyi Lin, Peng Jin, Kaipeng Zhang, et al. Sphinx-x: Scaling data and parameters for a family of  
 681 multi-modal large language models. *arXiv preprint arXiv:2402.05935*, 2024a.

682

683 Haotian Liu, Chunyuan Li, Qingyang Wu, and Yong Jae Lee. Visual instruction tuning. *Advances in*  
 684 *neural information processing systems*, 36:34892–34916, 2023.

685

686 Haotian Liu, Chunyuan Li, Yuheng Li, and Yong Jae Lee. Improved baselines with visual instruction  
 687 tuning. In *Proceedings of the IEEE/CVF Conference on Computer Vision and Pattern Recognition*,  
 688 pp. 26296–26306, 2024b.

689

690 Haotian Liu, Chunyuan Li, Yuheng Li, Bo Li, Yuanhan Zhang, Sheng Shen, and Yong Jae Lee.  
 691 Llava-next: Improved reasoning, ocr, and world knowledge, January 2024c. URL <https://llava-vl.github.io/blog/2024-01-30-llava-next/>.

692

693 Yuanxin Liu, Shicheng Li, Yi Liu, Yuxiang Wang, Shuhuai Ren, Lei Li, Sishuo Chen, Xu Sun,  
 694 and Lu Hou. Tempcompass: Do video llms really understand videos?, 2024d. URL <https://arxiv.org/abs/2403.00476>.

695

696 Muhammad Maaz, Hanooma Rasheed, Salman Khan, and Fahad Shahbaz Khan. Video-chatgpt:  
 697 Towards detailed video understanding via large vision and language models. *arXiv preprint*  
 698 *arXiv:2306.05424*, 2023.

699

700 Muhammad Maaz, Hanooma Rasheed, Salman Khan, and Fahad Shahbaz Khan. Videogpt+: In-  
 701 tegrating image and video encoders for enhanced video understanding. *arxiv*, 2024. URL  
 702 <https://arxiv.org/abs/2406.09418>.

703 Karttikeya Mangalam, Raiymbek Akshulakov, and Jitendra Malik. Egoschema: A diagnostic  
 704 benchmark for very long-form video language understanding. *Advances in Neural Information*  
 705 *Processing Systems*, 36:46212–46244, 2023.

702 Brandon McKinzie, Zhe Gan, Jean-Philippe Fauconnier, Sam Dodge, Bowen Zhang, Philipp Dufter,  
 703 Dhruti Shah, Xianzhi Du, Futang Peng, Anton Belyi, et al. Mm1: methods, analysis and insights  
 704 from multimodal llm pre-training. In *European Conference on Computer Vision*, pp. 304–323.  
 705 Springer, 2024.

706 Basil Mustafa, Carlos Riquelme, Joan Puigcerver, Rodolphe Jenatton, and Neil Houlsby. Multimodal  
 707 contrastive learning with limoe: the language-image mixture of experts. *Advances in Neural*  
 708 *Information Processing Systems*, 35:9564–9576, 2022.

709 Arsha Nagrani et al. Neptune: The long orbit to benchmarking long video understanding, 2025. URL  
 710 <https://arxiv.org/abs/2412.09582>.

711 OpenAI. Gpt-4 technical report, 2023.

712 Viorica Pătrăucean, Lucas Smaira, Ankush Gupta, Adrià Recasens Continente, Larisa Markeeva,  
 713 Dylan Banarse, Skanda Koppula, Joseph Heyward, Mateusz Malinowski, Yi Yang, Carl Do-  
 714 ersch, Tatiana Matejovicova, Yury Sulsky, Antoine Miech, Alex Frechette, Hanna Klimczak,  
 715 Raphael Koster, Junlin Zhang, Stephanie Winkler, Yusuf Aytar, Simon Osindero, Dima Damen,  
 716 Andrew Zisserman, and João Carreira. Perception test: A diagnostic benchmark for multi-  
 717 modal video models. In *Advances in Neural Information Processing Systems*, 2023. URL  
 718 <https://openreview.net/forum?id=HYEGXFnPoq>.

719 Qwen-Team. Qwen2 technical report, 2024. URL <https://arxiv.org/abs/2407.10671>.

720 Qwen-Team. Qwen2.5 technical report, 2025. URL <https://arxiv.org/abs/2412.15115>.

721 Kanchana Ranasinghe, Xiang Li, Kumara Kahatapitiya, and Michael S Ryoo. Understanding long  
 722 videos with multimodal language models. *arXiv preprint arXiv:2403.16998*, 2024.

723 Ruchit Rawal, Khalid Saifullah, Miquel Farré, Ronen Basri, David Jacobs, Gowthami Somepalli, and  
 724 Tom Goldstein. Cinepile: A long video question answering dataset and benchmark. *arXiv preprint*  
 725 *arXiv:2405.08813*, 2024.

726 Carlos Riquelme, Joan Puigcerver, Basil Mustafa, Maxim Neumann, Rodolphe Jenatton, André  
 727 Susano Pinto, Daniel Keysers, and Neil Houlsby. Scaling vision with sparse mixture of experts.  
 728 *Advances in Neural Information Processing Systems*, 34:8583–8595, 2021.

729 Share. Sharegemini: Scaling up video caption data for multimodal large language models, June 2024.  
 730 URL <https://github.com/Share14/ShareGemini>.

731 Reuben Tan, Ximeng Sun, Ping Hu, Jui-hsien Wang, Hanieh Deilamsalehy, Bryan A Plummer, Bryan  
 732 Russell, and Kate Saenko. Koala: Key frame-conditioned long video-llm. In *Proceedings of the*  
 733 *IEEE/CVF Conference on Computer Vision and Pattern Recognition*, pp. 13581–13591, 2024.

734 Chau Tran, Duy MH Nguyen, Manh-Duy Nguyen, TrungTin Nguyen, Ngan Le, Pengtao Xie, Daniel  
 735 Sonntag, James Y Zou, Binh Nguyen, and Mathias Niepert. Accelerating transformers with  
 736 spectrum-preserving token merging. *Advances in Neural Information Processing Systems*, 37:  
 737 30772–30810, 2024.

738 Haoning Wu, Dongxu Li, Bei Chen, and Junnan Li. Longvideobench: A benchmark for long-context  
 739 interleaved video-language understanding, 2024a. URL <https://arxiv.org/abs/2407.15754>.

740 Yuanchen Wu, Junlong Du, Ke Yan, Shouhong Ding, and Xiaoqiang Li. Tove: Efficient vision-  
 741 language learning via knowledge transfer from vision experts, 2025. URL <https://arxiv.org/abs/2504.00691>.

742 Zhiyu Wu et al. Deepseek-vl2: Mixture-of-experts vision-language models for advanced multimodal  
 743 understanding, 2024b. URL <https://arxiv.org/abs/2412.10302>.

744 Junbin Xiao, Xindi Shang, Angela Yao, and Tat-Seng Chua. Next-qa:next phase of question-answering  
 745 to explaining temporal actions, 2021. URL <https://arxiv.org/abs/2105.08276>.

756 Zhengzhuo Xu, Bowen Qu, Yiyan Qi, Sinan Du, Chengjin Xu, Chun Yuan, and Jian Guo. Chartmoe:  
 757 Mixture of expert connector for advanced chart understanding. *arXiv preprint arXiv:2409.03277*,  
 758 2024.

759 Jingkang Yang et al. Egolife: Towards egocentric life assistant, 2025. URL <https://arxiv.org/abs/2503.03803>.

760 Zhengyuan Yang, Linjie Li, Kevin Lin, Jianfeng Wang, Chung-Ching Lin, Zicheng Liu, and Li-  
 761 juan Wang. The dawn of lmms: Preliminary explorations with gpt-4v (ision). *arXiv preprint*  
 762 *arXiv:2309.17421*, 9(1):1, 2023.

763 Shoubin Yu, Jaemin Cho, Prateek Yadav, and Mohit Bansal. Self-chained image-language model for  
 764 video localization and question answering. *Advances in Neural Information Processing Systems*,  
 765 36:76749–76771, 2023.

766 Zhou Yu, Dejing Xu, Jun Yu, Ting Yu, Zhou Zhao, Yuetong Zhuang, and Dacheng Tao. Activitynet-qa:  
 767 A dataset for understanding complex web videos via question answering. In *AAAI*, pp. 9127–9134,  
 768 2019.

769 Xiangyu Zeng, Kunchang Li, Chenting Wang, Xinhao Li, Tianxiang Jiang, Ziang Yan, Songze  
 770 Li, Yansong Shi, Zhengrong Yue, Yi Wang, et al. Timesuite: Improving mllms for long video  
 771 understanding via grounded tuning. *arXiv preprint arXiv:2410.19702*, 2024.

772 Jihai Zhang, Xiaoye Qu, Tong Zhu, and Yu Cheng. Clip-moe: Towards building mixture of experts  
 773 for clip with diversified multiplet upcycling, 2024a. URL <https://arxiv.org/abs/2409.19291>.

774 Kaichen Zhang et al. Lmms-eval: Reality check on the evaluation of large multimodal models. In  
 775 *Findings of the Association for Computational Linguistics: NAACL 2025*, pp. 881–916. Association  
 776 for Computational Linguistics, 2025. doi: 10.18653/v1/2025.findings-naacl.51. URL <http://dx.doi.org/10.18653/v1/2025.findings-naacl.51>.

777 Yuanhan Zhang, Bo Li, haotian Liu, Yong jae Lee, Liangke Gui, Di Fu, Jiashi Feng, Ziwei Liu, and  
 778 Chunyuan Li. Llava-next: A strong zero-shot video understanding model, April 2024b. URL  
 779 <https://llava-vl.github.io/blog/2024-04-30-llava-next-video/>.

780 Yuanhan Zhang, Jinming Wu, Wei Li, Bo Li, Zejun Ma, Ziwei Liu, and Chunyuan Li. Video instruc-  
 781 tion tuning with synthetic data, 2024c. URL <https://arxiv.org/abs/2410.02713>.

782 Junjie Zhou, Yan Shu, Bo Zhao, Boya Wu, Shitao Xiao, Xi Yang, Yongping Xiong, Bo Zhang,  
 783 Tiejun Huang, and Zheng Liu. Mlvu: A comprehensive benchmark for multi-task long video  
 784 understanding. *arXiv preprint arXiv:2406.04264*, 2024.

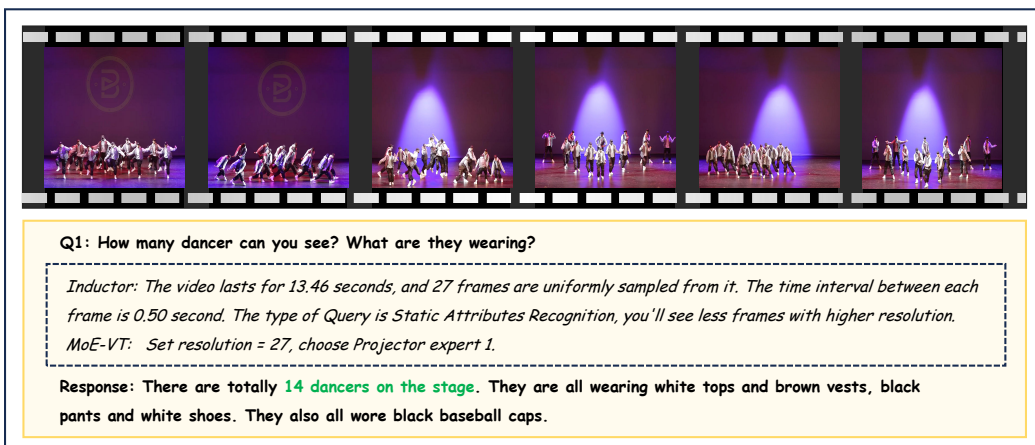
785 Barret Zoph, Irwan Bello, Sameer Kumar, Nan Du, Yanping Huang, Jeff Dean, Noam Shazeer, and  
 786 William Fedus. St-moe: Designing stable and transferable sparse expert models, 2022. URL  
 787 <https://arxiv.org/abs/2202.08906>.

788  
 789  
 790  
 791  
 792  
 793  
 794  
 795  
 796  
 797  
 798  
 799  
 800  
 801  
 802  
 803  
 804  
 805  
 806  
 807  
 808  
 809

810 A MORE DETAILS ABOUT TRAINING DATA COLLECTING  
811812 A.1 TAGGING PROMPTS  
813814 To train the classification capability for different tasks of Inductor, we selected 116K high-quality,  
815 non-redundant queries (excluding answers) from open-source datasets. Subsequently, we annotated  
816 these data using the Deepseek-R1 model, ultimately forming the TA-116K dataset. For clarity, we  
817 present the prompts in tabular form. The content of our prompts is as follows.  
818819 Generally, the video understanding tasks can be categorized into  
820 the following eight types:  
821822 Table 7: The Prompts and Description in Tagging, Describing Our Classification Strategies to Deepseek-R1.  
823

Category	Description	Example
<b>Static Attributes Recognition</b>	Identifying perceptible static attributes of people/objects (color, quantity, state, material, etc.), or existence queries. Includes object retrieval and counting problems.	<ul style="list-style-type: none"> <li><i>- What color is the helicopter?</i></li> <li><i>- How many riders are on the podium?</i></li> <li><i>- How many people are there in the video?</i></li> </ul>
<b>Action Recognition</b>	Recognizing dynamic events/actions and interaction relationships (excluding facial expressions). Includes methods of achieving actions.	<ul style="list-style-type: none"> <li><i>- What does the person do after opening a can of chickpeas?</i></li> <li><i>- How does the skier move down the slope?</i></li> <li><i>- How did the man make his way to his home?</i></li> </ul>
<b>Fine-grained Attributes Recognition</b>	Identifying advanced attributes like poses, emotions, and facial expressions, typically requiring subtitle/dialogue analysis.	<ul style="list-style-type: none"> <li><i>- Does the man feel sorry for the woman?</i></li> <li><i>- Is the woman happy or angry at the end of the video?</i></li> </ul>
<b>Temporal Sequence Positioning</b>	Determining event sequences/timings, causal order, or occurrence counts (limited to video content).	<ul style="list-style-type: none"> <li><i>- Arrange the events in chronological order.</i></li> <li><i>- What happened after the man left the house?</i></li> <li><i>- How many times did the brightness change?</i></li> </ul>
<b>Spatial Orientation and Navigation</b>	Recognizing positions/spatial relationships or navigation sequences in environments.	<ul style="list-style-type: none"> <li><i>- Where is the yellow container located?</i></li> <li><i>- Where is the kitchen, next to the bedroom or next to the washroom?</i></li> </ul>
<b>Summary and Generalization</b>	Extracting narrative structures, themes, or actionable insights through content summarization.	<ul style="list-style-type: none"> <li><i>- Analyze the video's narrative structure.</i></li> <li><i>- What's the video mainly about?</i></li> <li><i>- According to the video, how can we solve the problem?</i></li> </ul>
<b>Reasoning and Logic</b>	Inferring causes, motivations, purposes, or relationships between entities based on video content.	<ul style="list-style-type: none"> <li><i>- Why did the toddler cry at the end?</i></li> <li><i>- What indicates that the food is being cooked?</i></li> <li><i>- What made the man angry?</i></li> <li><i>- Is their relationship more like friend or enemy?</i></li> </ul>
<b>OCR and Cross-modal Alignment</b>	Cross-modal alignment between video content and text (e.g., subtitle matching), or identifying on-screen text.	<ul style="list-style-type: none"> <li><i>- What objects appear after the subtitle mentions 'multiple reasons'?</i></li> <li><i>- Match the dialogue to the scene.</i></li> </ul>

859 You can take answer options into account when available. Ignore  
860 non-semantic content (e.g., "Answer using short words") when  
861 analyzing questions.  
862

864 A.2 CLASSIFICATION STRATEGY  
865866 As shown in Tab. 7 in Appendix A.1, we divide video understanding tasks into eight types. Our main  
867 classification criteria are the inherent meaning of the tasks and their different sensitivities to frame  
868 count and resolution. When considering only the sensitivity to these two factors, the tasks can be  
869 categorized into the following three groups:870 1. Tasks more sensitive to resolution: tasks that depend on fine details, such as Static Attributes  
871 Recognition, Spatial Orientation and Navigation, and retrieval counting, are sensitive to  
872 resolution. MoE-VT will provide inputs with less frames but higher resolution.  
873 2. Tasks more sensitive to frame count: tasks like Temporal sequence positioning, retrieval  
874 counting, and Summary and Generalization become significantly more complex in long  
875 videos. MoE-VT will provide inputs with more frames but lower resolution.  
876 3. Balanced tasks: some tasks may span multiple categories. For example, a Reasoning  
877 and Logic task might involve aspects of Action Recognition along with logical reasoning.  
878 MoE-VT will provide inputs with a balanced number of frames and resolution.  
879880 B DATASET COMPOSITION  
881882 In the main text of the paper, we have already presented the composition and proportion of the training  
883 data used in Stage 2 and Stage 3. To maximize the extent to which our progress is not solely due  
884 to the data, we used almost the same data as in the baseline for training. To prevent overfitting, we  
885 also utilize partial samples from the EgoIT-99K Yang et al. (2025) and NeptuneNagrani et al. (2025)  
886 datasets, which make up no more than a quarter of our training dataset.  
887888 In the attached code package, readers can also find the specific data proportions for these stages  
889 stored in files such as "./scripts/TallVA/all\_data\_stagex.yaml". Please refer to the code if needed.  
890891 C ADDITIONAL REPRESENTATIVE CASE STUDIES  
892893 In the main text of the paper (Fig. 8), we demonstrated the performance of TallVA on two distinct  
894 styles of tasks and compared it with a baseline model, showcasing the strong adaptability across  
895 different tasks. To further highlight the comprehensive capabilities of TallVA, we provide additional  
896 case studies here. For consistency with the main text, we highlight **correct content** and **incorrect**  
897 **content** with different color. We also visualized the output of Inductor and MoE-VT. However,  
898 it should be noted that the Inductor outputs only the task type, while the figure shows the Task  
899 Instructions added to the LLM.  
900916 Figure 9: **Case Study on Short Clips.** For shorter videos, TallVA is able to utilize higher resolution frames to  
917 help understand the detailed content of the video.

918  
919  
920  
921  
922  
923  
924  
925  
926  
927  
928  
929  
930  
931  
932  
933  
934  
935  
936  
937  
938  
939  
940  
941  
942  
943  
944  
945  
946  
947  
948  
949  
950  
951  
952  
953  
954  
955  
956  
957  
958  
959  
960  
961  
962  
963  
964  
965  
966  
967  
968  
969  
970  
971


**Q1: What is the video mainly about? Describe the video.**

*Inductor: The video lasts for 1786.30 seconds, and 120 frames are uniformly sampled from it. The time interval between each frame is 15.10 second. The type of Query is Summary & Generalization, you'll see more frames and lower resolution.*

*MoE-VT: Set resolution = 11, choose Projector expert 4.*

**Response:** The video is about the wild animals. It opens with a serene scene of a herd of wildebeests grazing in a grassy field, transitioning to various other animals such as rhinoceroses, lions, cheetahs, and elephants. The narrative continues with close-ups of birds like toucans, macaws, and parrots, followed by scenes of flamingos, a porcupine, and a sloth. The focus shifts to a giraffe, a bear, and a gorilla, highlighting their natural habitats. The video then showcases a variety of birds, including ostriches, eagles, and penguins, followed by marine life like whales and sharks. The narrative returns to terrestrial scenes with zebras, buffaloes, and antelopes, concluding with a majestic view of a lion and a leopard. The final segment features a diverse array of animals, including camels, hippos, and a large group of wildebeests, emphasizing the richness and diversity of wildlife across different environments.

**Q2: Is the video about wild animals in Africa? Explain why in detail.**

*Inductor: The video lasts for 1786.30 seconds, and 120 frames are uniformly sampled from it. The time interval between each frame is 15.10 second. The type of Query is Reasoning & Logic, you'll see balanced frames and resolution.*

*MoE-VT: Set resolution = 11, choose Projector expert 4.*

**Response:** No, it is about wild animals from different continents. The video showcases a diverse range of wildlife from various regions, including Africa, Asia, and the Americas. The video shows penguins, which are unlikely to be found in Africa.



**Q1: What happened in the video?**

*Inductor: The video lasts for 77.43 seconds, and 78 frames are uniformly sampled from it. The time interval between each frame is 1.00 second. The type of Query is Summary & Generalization, you'll see more frames with lower resolution.*

*MoE-VT: Set resolution = 14, choose Projector expert 3.*

**Response:** A panda character enters a grand, dimly lit hall adorned with green, vine-like columns and intricate golden decorations. The panda, wearing a black and white outfit with a yellow belt, explores the hall, examining various objects including a large, ornate sword and a golden vase with a dragon design. The panda's curiosity and excitement are evident as it interacts with these items. Eventually, the panda accidentally drops the vase, causing it to shatter into pieces. The panda looks distressed and is approached by another character dressed in brown with a white face and blue eyes, who appears to be scolding the panda.

**Q2: What was the master's reaction after seeing the panda?**

*Inductor: The video lasts for 77.43 seconds, and 51 frames are uniformly sampled from it. The time interval between each frame is 1.51 second. The type of Fine-grained Recognition, you'll see less frames with higher resolution.*

*MoE-VT: Set resolution = 18, choose Projector expert 2.*

**Response:** He looks very angry because the panda broke the porcelain, perhaps that porcelain has a high value.

Figure 10: **More Case Studies of Different Styles Videos.** We demonstrated realistic style ultra-long videos, as well as 3D animations. TallVA shows better performance on different styles of videos.

972  
973  
974  
975  
976  
977  
978  
979  
980  
981  
982  
983  
984  
985  
986  
987  
988  
989  
990  
991  
992  
993  
994  
995  
996  
997  
998  
999  
1000  
1001  
1002  
1003  
1004  
1005  
1006  
1007  
1008  
1009  
1010  
1011  
1012  
1013  
1014  
1015  
1016  
1017  
1018  
1019  
1020  
1021  
1022  
1023  
1024  
1025

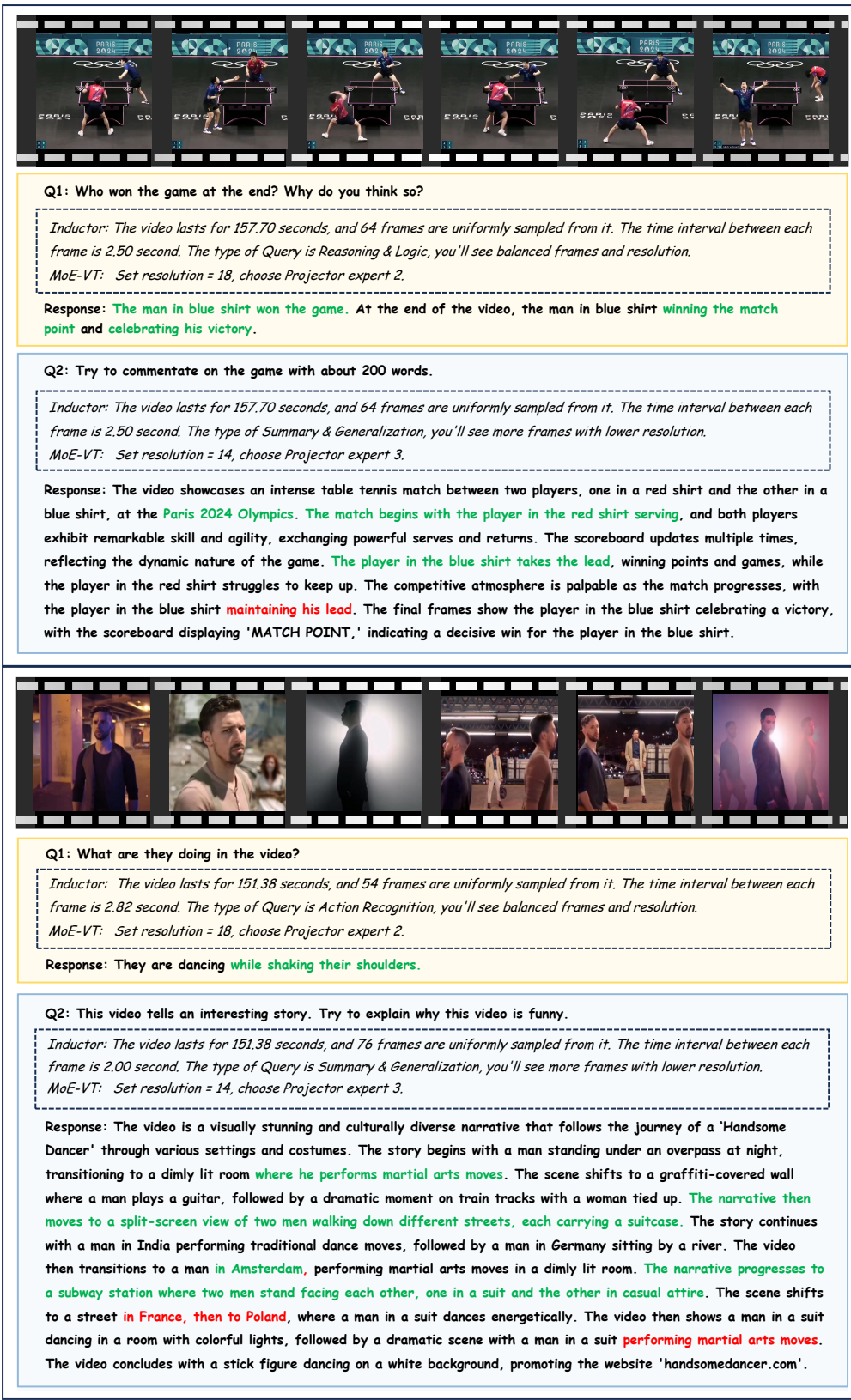


Figure 11: **Case Studies for Deeper Understanding of Plot and Content.** We found that TallVA may have some hallucinations on problems with high difficulty. To solve this problem, we suggest using more complete dataset with a more powerful LLM in the future.

1026 These cases are categorized into three groups. Short videos that focus on fine details in Fig. 9; videos  
 1027 with completely different styles (including 3D animations that were not present in the training data)  
 1028 in Fig. 10; the deeper understanding of plots and content, involving more human-like activities such  
 1029 as match commentary or watching a funny video in Fig. 11.  
 1030

## D DISCUSSION: FUTURE DIRECTIONS AND DESIGN CONSIDERATIONS

1034 In this section, we discuss three design questions that arose during the development of TAM: the  
 1035 relationship between task-aware routing and difficulty estimation, the compatibility with token  
 1036 compression methods, and the role of hard-coded routing in future LVLM design.  
 1037

### D.1 TAM AND DIFFICULTY-AWARE ROUTING

1040 A natural question is whether TAM should incorporate sample-wise difficulty estimation to allocate  
 1041 visual budgets more precisely. We carefully considered this direction and concluded that, while  
 1042 intuitive, difficulty-based routing faces fundamental challenges for video understanding.  
 1043

1044 The core problem is that understanding “what makes a question hard” is closely related to answering  
 1045 it. Existing difficulty estimation methods mainly fall into two categories, neither of which works  
 1046 well for our setting. Model cascade approaches—running a weak model first and marking failures as  
 1047 “hard”—require multiple forward passes through large models, exactly what we want to avoid with a  
 1048 lightweight Inductor. Heuristic approaches like modeling frame-to-frame entropy completely ignore  
 1049 the user query; yet the same video can be trivial (“What color is the car?”) or extremely hard (“Count  
 1050 all people in the background”) depending on what is asked.  
 1051

1052 Even if we had a reliable difficulty score, translating it into frame count and resolution decisions is  
 1053 non-trivial. Consider that for a 2-hour movie, “What is the weather like?” is easy—a few frames  
 1054 suffice—while for a 10-second clip, “How many plants are on the lawn?” might be very hard,  
 1055 requiring high-resolution frames and careful counting. Moreover, a “hard” OCR question needs  
 1056 higher resolution, whereas a “hard” temporal reasoning question needs more frames. A single  
 1057 difficulty score cannot tell us *where* to spend the budget. This is fundamentally different from  
 1058 text-only tasks, where we can often improve performance on hard questions by giving the model  
 1059 more “thinking time.” For video understanding, if we missed the key frame, no amount of reasoning  
 1060 will recover the lost information.  
 1061

1062 Given these challenges, TAM takes a pragmatic approach: rather than chasing sample-wise difficulty,  
 1063 we classify queries into task types that reflect different patterns of frame-count and resolution  
 1064 requirements. Within each type, the actual budget still varies with video length (see Figures 8–11 in  
 1065 Appendix C). Our experiments demonstrate that this simple task-aware and length-aware scheme  
 1066 already yields substantial gains.  
 1067

1068 That said, we do see a role for difficulty estimation in future work. The key insight is that difficulty  
 1069 might be better used to allocate *reasoning* budgets rather than *visual* budgets. One could imagine  
 1070 a system where TAM handles the visual side, and a separate module decides how much chain-of-  
 1071 thought or iterative refinement to apply based on query difficulty. Reasoning-centric multimodal  
 1072 models remain underexplored, and TAM may serve as a foundation that could later be combined with  
 1073 difficulty-aware reasoning modules.  
 1074

### D.2 TAM AND TOKEN COMPRESSION METHODS

1075 Several recent works have proposed token pruning or token merging to reduce the number of visual  
 1076 tokens fed to the LLM. We clarify how TAM relates to these approaches and discuss their potential  
 1077 combination.  
 1078

1079 First, we explain how TAM controls token count. Taking SigLIP-so400m-patch14 as an example,  
 1080 each frame is divided into  $27 \times 27$  patches, which are then pooled via bilinear interpolation. By  
 1081 changing the pooling stride, we control how many patches each frame produces: stride 2 yields  
 1082  $14 \times 14 = 196$  patches (default), stride 1 yields  $27 \times 27 = 729$  patches (highest resolution), and  
 1083 stride 3 yields  $9 \times 9 = 81$  patches (lower resolution). Each patch becomes one token after the ViT.  
 1084

1080 Thus, TAM controls token count at the *video level*, before frames even enter the ViT, by deciding  
 1081 how many frames to sample and at what resolution.  
 1082

1083 Token pruning and merging methods work differently. These approaches operate *inside* the ViT, using  
 1084 attention scores or learned importance weights to drop or merge tokens from a fixed-resolution input.  
 1085 They reduce redundancy within the selected frames but do not consider task-level requirements.  
 1086

1087 Structurally, the two approaches are complementary rather than competing. TAM asks: “Given this  
 1088 query and video, how many frames do we need, and at what resolution?” Token pruning asks: “Given  
 1089 these frames, which patches are actually important?” There is no conflict between these questions.  
 1090 In fact, combining them could yield even better efficiency: TAM first decides the frame budget and  
 1091 resolution based on the query and video length, and then token pruning further compresses within  
 1092 those frames.  
 1093

1094 Due to resource constraints, we could not run full experiments on this combination during the current  
 1095 work, but we believe it is a promising direction. Both approaches share the goal of improving LVLMs  
 1096 from the vision side, rather than solely relying on LLM modifications.  
 1097

### 1097 D.3 THE ROLE OF HARD-CODED ROUTING

1099 One might view TAM’s use of predefined routing rules as a limitation—should we not learn everything  
 1100 end-to-end? We argue that hard-coded routing is actually a reasonable design choice for the current  
 1101 stage of research, and we explain our reasoning below.  
 1102

1103 First, we emphasize that TAM is not purely hard-coded but employs a *hybrid* gating strategy. The  
 1104 MoE-ViT uses soft routing where experts are selected based on learned gates. The MoE-Projector  
 1105 uses hard routing based on resolution. Frame count and resolution are determined by task type  
 1106 and video length via predefined rules. Our ablations (Table 3 in the main paper) show that this  
 1107 combination works better than using soft or hard routing uniformly—different components benefit  
 1108 from different strategies.  
 1109

1110 Why not learn frame count and resolution end-to-end? We considered this carefully, but there are  
 1111 practical obstacles. Current ViT architectures like SigLIP and CLIP are not designed for variable-  
 1112 resolution inputs in a differentiable way. We would need massive amounts of data annotating “the  
 1113 right frame count and resolution for this query,” which does not exist. Furthermore, frame sampling  
 1114 is inherently discrete—you cannot sample 16.5 frames—making gradient-based learning difficult.  
 1115 Hard-coded rules allow us to validate the core idea that task-aware visual budgeting helps, without  
 1116 needing to solve all these challenges simultaneously.  
 1117

1118 For practical deployment, hard-coded routing offers several advantages. The Inductor can be trained  
 1119 independently and frozen during LVLM training. Routing rules can be quickly tested and adjusted  
 1120 without retraining the whole model. Resource usage is predictable, which is important for edge  
 1121 devices with limited memory. The system’s behavior is also interpretable: developers can understand  
 1122 why a particular frame count was chosen for a given query.  
 1123

1124 We view this work as a stepping stone rather than the final answer. The research trajectory we envision  
 1125 proceeds as follows: first, validate that task-aware budgeting helps using simple rules (this work);  
 1126 then, explore learned routers that can optimize frame and resolution selection jointly; eventually,  
 1127 develop fully differentiable pipelines that can adapt to new task types without manual intervention.  
 1128 TAM establishes that the *goal*—adapting visual processing to the task—is worthwhile. The specific  
 1129 *mechanism* (hard vs. soft routing) is a design choice that can evolve as the field matures.  
 1130

### 1128 D.4 BROADER IMPACTS

1131 Our approach enhances the ability of LVLMs to understand video content by providing task-  
 1132 appropriate visual inputs, contributing to more capable multimodal AI systems. Open-source weights  
 1133 and code can accelerate community development, though they may also carry potential risks. We  
 1134 have added appropriate licenses to guide responsible use of our model.  
 1135

1134 **E TRAINING SETS AND HYPERPARAMETERS**  
1135

1136 Tab. 8 shows our specific hyperparameter settings for Training Stages 2 and 3. We used the same  
 1137 learning rate (LR) and LR scheduler for both stages. We employed the AdamW optimizer with a  
 1138 batch size of 1, gradient accumulation of 2, and 16 GPUs using Zero1-offload and Zero2-offload. The  
 1139 Vision Encoder and Projector were frozen while the LLM was trained. Additionally, we incorporated  
 1140 MoE Blocks to enhance the model’s capacity. The maximum context length (including visual tokens  
 1141 and text tokens) is set to 21000. **Training takes about 1.5k A100 GPU hours in total for Stages**  
 1142 **2–3.** For further details, please refer to Tab. 8.

1143  
1144 Table 8: Hyperparameters for the second and third stages of training.  
1145

Hyperparameter	Stage 2	Stage 3
<b>Learning Rate</b>	$2.5e - 5$	$2.5e - 5$
<b>Vision Tower LR</b>	–	$5e - 6$
<b>LR schedule</b>	Cosine	Cosine
<b>Batchsize per GPU</b>	1	1
<b>Gradient Acc.</b>	2	2
<b>GPU Number</b>	$16 \times A100$	$16 \times A100$
<b>Zero</b>	Zero1-offload	Zero2-offload
<b>Optimizer</b>	AdamW	AdamW
<b>Projector</b>	Freeze	Train
<b>Vision Encoder</b>	Freeze	Train
<b>LLM</b>	Train	Train
<b>MoE Blocks</b>	–	✓
<b>Max Context Length</b>	21000	21000
<b>Max Output Token</b>	2048	2048
<b>Warm Up Ratio</b>	0.03	0.03
<b>Total Steps</b>	1200	3200

1166 **F OPEN-SOURCE MODEL WEIGHTS AND CODE**  
1167

1168 To support reproducibility and further research, we provide the full implementation code in the  
 1169 supplementary materials under the file code.zip. This package includes the core modules, training  
 1170 scripts, and documentation necessary to replicate our experiments. Please note that this is a prelimi-  
 1171 nary release intended for review purposes; the codebase will be further cleaned, documented, and  
 1172 restructured prior to public release.

1173 In addition, model weights and checkpoints will be made publicly available after the conclusion. We  
 1174 are committed to open science and plan to release the weights alongside the finalized code repository,  
 1175 ensuring full transparency and ease of use for the research community.

1176 We use the lmms-eval suite Zhang et al. (2025) for evaluation, but we have modified these scripts to  
 1177 meet the requirements of TallVA. Specifically, the startup script can be found in “./script/”.

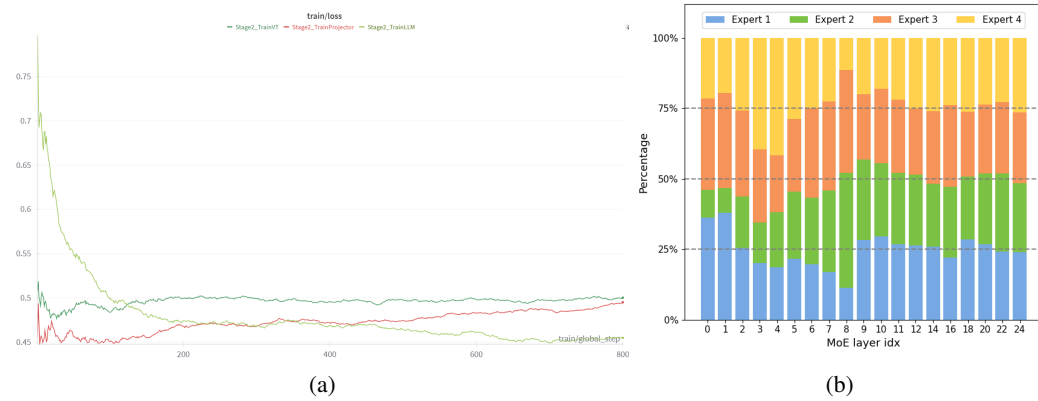
1180 **G LIMITATIONS**  
1181

1182 Due to time and resource constraints, we only tested TAM on the 7B model and did not verify its  
 1183 effectiveness on larger models with longer contexts. Secondly, as a video understanding model,  
 1184 TallVA still exhibits hallucination issues, with additional successful and failed cases presented in  
 1185 Appendix C. In future work, we will evaluate TAM on larger models and attempt to collect more data  
 1186 to optimize the classification strategy. We believe that applying TAM to models with longer context  
 1187 lengths(such as 128k tokens) will yield even better performance.

## 1188 H LOSS ANALYSIS IN TRAINING STAGE 2 1189

1190 In the main text, we mentioned that "our extensive experiments prove that the LLM should be trained  
1191 first in Stage 2." We believe that this is effective because the application of Dynamic Frames Number  
1192 and Resolution has the greatest impact on the LLM. Therefore, the LLM needs to learn how to  
1193 handle varying numbers and resolutions of frames first; otherwise, errors will accumulate in the LLM,  
1194 ultimately making it difficult to train the Vision Tower.

1195 To validate our hypothesis, we present the loss curves in Fig. 12a of different training strategies in  
1196 Stage 2. We selected three typical scenarios: training the LLM first, training the Projector first, or  
1197 training the entire VT (Vision Encoder + Projector). As shown in Tab. 3, the loss curve of LMM-  
1198 Training decreases rapidly at the beginning of training, whereas the other two approaches exhibit an  
1199 upward trend in loss along with a significant drop in actual performance.



1200  
1201  
1202  
1203  
1204  
1205  
1206  
1207  
1208  
1209  
1210  
1211  
1212  
1213  
1214 Figure 12: **Training and Visualization Analysis.** (a) Loss analysis in Stage 2; (b) MoE VE layer-wise  
1215 visualization with load balancing.

## 1217 I ADDITIONAL EXPERIMENTS AND ANALYSIS 1218

1219 This section provides supplementary experiments referenced in the main paper, including MoE  
1220 isolation studies, expert interchangeability tests, task extensibility, and accuracy–efficiency tradeoff  
1221 analysis.

### 1223 I.1 MOE ISOLATION STUDY 1224

1225 As discussed in Section 4.3, we investigate whether performance gains stem from MoE capacity  
1226 or query-aware routing. Tab. 9 shows that simply replacing the vision encoder with an MoE-ViT  
1227 (without Dynamic Frames and Resolution) leads to performance degradation across all configurations.

1228  
1229 **Table 9: Impact of MoE-ViT Isolation (without DFR).** We evaluated MoE-ViT configurations while keeping  
1230 the LLM and projector fixed. The results indicate that simply replacing the vision encoder with an MoE-ViT  
1231 (without query-aware routing) leads to performance degradation across benchmarks.

Model	Baseline	Top2 in 8	Top2 in 4	Top1 in 4
Videomme	63.3	61.5	62.8	63.0
MVBF	58.6	53.3	56.7	56.5
MLVU-Test	44.8	42.0	43.5	42.2
Relative Avg Change	+0%	-5.98%	-2.21%	-3.01%

1232  
1233  
1234  
1235  
1236  
1237  
1238  
1239  
1240 This result aligns with prior work Li et al. (2024b) showing that MoE-izing the vision encoder alone  
1241 does not automatically yield gains. The MoE experts require task-appropriate visual inputs (enabled  
1242 by DFR) to specialize effectively.

1242 **I.2 EXPERT INTERCHANGEABILITY TESTS**  
12431244 To verify that MoE routing is causally important, we performed expert-swap and routing-scramble  
1245 experiments.  
12461247 **Table 10: Causal Analysis of MoE-ViT Routing.** We compare standard routing against Random Top-2 and  
1248 Lowest-2 selection. The significant performance drop (up to 12.5%) confirms that the learned router identifies  
1249 necessary experts rather than selecting arbitrarily.  
1250

MoE-ViT Configuration	Videomme	MVBench	Relative Avg Change
Normal TAM	65.6	64.5	+0%
Random Top-2	60.3	58.2	-9.8%
Lowest 2 Experts	56.1	55.7	-12.5%

1257 **Table 11: Causal Analysis of MoE-Projector Routing.** Since the Projector uses hard-gating based on resolution,  
1258 we test *Random* mapping and *Expert Swap* (swapping high-res and low-res experts). The drastic drop (−13.6%)  
1259 in Expert Swap confirms that experts are highly specialized for specific resolutions.  
1260

MoE-Projector Config	Videomme	MVBench	Relative Avg Change
Normal TAM	65.6	64.5	+0%
+Random Experts	63.2	62.7	-3.2%
+Expert Swap	58.3	54.1	-13.6%

1266 For MoE-ViT (Tab. 10), Random Top-2 selection degrades performance by 9.8%, and selecting the  
1267 Lowest-2 experts causes 12.5% degradation. For MoE-Projector (Tab. 11), swapping the highest-  
1268 resolution and lowest-resolution experts leads to 13.6% degradation. These results confirm that  
1269 both the learned routing in MoE-ViT and the resolution-expert mapping in MoE-Projector are  
1270 essential—experts are *not* interchangeable.  
12711273 **I.3 LOW-COST TASK EXTENSIBILITY**1275 To demonstrate that TAM can flexibly adapt to new requirements, we defined a new “very-long-video”  
1276 task type using approximately 800 samples and fine-tuned only the 135M Inductor via LoRA (2  
1277 epochs), keeping the full LVLM frozen.  
12781279 **Table 12: Low-Cost Extensibility via Inductor Adaptation.** We defined a new task type (“very-long-video”)  
1280 using ∼800 samples and fine-tuned only the 135M Inductor via LoRA. This minimal adaptation yielded clear  
1281 gains on long-video benchmarks (Videomme, LongVideoBench), demonstrating that TAM can flexibly adapt to  
1282 new requirements without retraining the full LVLM.  
1283

Inductor Configuration	Videomme (Long)	LongVideoBench (Long)	NextQA (Short)
Original Inductor	65.6	59.6	84.0
Inductor after LoRA Finetune	<b>66.2</b>	<b>60.8</b>	82.7

1288 As shown in Tab. 12, this minimal adaptation yields clear gains on long-video benchmarks (Videomme  
1289 +0.6, LongVideoBench +1.2) with a slight trade-off on short videos. This confirms that new task  
1290 types can be added at very low cost without retraining the full model.  
12911292 **I.4 ACCURACY-EFFICIENCY TRADEOFF DETAILS**  
12931294 As shown in Tab. 5(c) in the main paper, we evaluated the Accuracy–FLOPs tradeoff by varying  
1295 frame counts and patch resolutions on samples from LongVideoBench and MLVU. The detailed  
1296 operating points are:  
1297

1296  
1297 Table 13: **Accuracy–FLOPs tradeoff of TallVA and Baseline.** We selected representative points from a series  
1298 of data that demonstrate TAM has better efficiency.

1299	<i>Baseline FLOPs</i>	$1.32 \times 10^{15}$	$1.55 \times 10^{15}$	$1.84 \times 10^{15}$ ( <i>Default</i> )	$2.54 \times 10^{15}$	$3.39 \times 10^{15}$
1300	<i>Baseline Acc</i>	39.5%	50.3%	58.7%	62.5%	63.8%
1301	<i>TallVA FLOPs</i>	$1.38 \times 10^{15}$	$1.72 \times 10^{15}$	$1.97 \times 10^{15}$ ( <i>Default</i> )	$2.62 \times 10^{15}$	$3.55 \times 10^{15}$
1302	<i>TallVA Acc</i>	50.5%	61.7%	63.6%	65.8%	66.7%

1304  
1305 At default settings, TallVA uses  $1.97 \times 10^{15}$  FLOPs compared to the baseline’s  $1.84 \times 10^{15}$  FLOPs  
1306 (+7%), while achieving significantly higher accuracy (63.3% vs 59.7%). Wall-clock latency follows  
1307 similar trends: 6.2s vs 5.7s per sample; peak memory is 61.2GB vs 57.5GB.  
1308

1309  
1310  
1311  
1312  
1313  
1314  
1315  
1316  
1317  
1318  
1319  
1320  
1321  
1322  
1323  
1324  
1325  
1326  
1327  
1328  
1329  
1330  
1331  
1332  
1333  
1334  
1335  
1336  
1337  
1338  
1339  
1340  
1341  
1342  
1343  
1344  
1345  
1346  
1347  
1348  
1349